สมบัติของฟิล์มเป่าพอลิแลคติกเอซิดผสมยางธรรมชาติและเทอร์โมพลาสติกสตาร์ช

นางสาวหนึ่งฤทัย ใจตรง

วิทยานิพนธ์นี้เป็นส่วนหนึ่งของการศึกษาตามหลักสูตรปริญญาวิศวกรรมศาสตรมหาบัณฑิต
สาขาวิชาวิศวกรรมเคมี ภาควิชาวิศวกรรมเคมี
คณะวิศวกรรมศาสตร์ จุฬาลงกรณ์มหาวิทยาลัย
ปีการศึกษา 2556

PROPERTIES OF POLY(LACTIC ACID)/NATURAL RUBBER/THERMOPLASTIC STARCH BLOWN FILMS

Miss Nuengruthai Jaitrong

A Thesis Submitted in Partial Fulfillment of the Requirements
for the Degree of Master of Engineering Program in Chemical Engineering
Department of Chemical Engineering
Faculty of Engineering
Chulalongkorn University
Academic Year 2013

Thesis Title	PROPERTIES OF POLY(LACTIC ACID)/NATURAL RUBBER/THERMOPLASTIC STARCH BLOWN FILMS
By	Miss Nuengruthai Jaitrong
Field of Study	Chemical Engineering
Thesis Advisor	Associate Professor Anongnat Somwangthanaroj, Ph.D.
Thesis Co-Advisor	Assistant Professor Wanchai Lerdwijitjarud, Ph.D.

Accepted by the Faculty of Engineering, Chulalongkorn University in Partial Fulfillment of the Requirements for the Master's Degree

.....Dean of the Faculty of Engineering

(Professor Bundhit Eua-arporn, Ph.D.)

THESIS COMMITTEE

.....Chairman

(Associate Professor Siriporn Damrongsakkul, Ph.D.)

.....Thesis Advisor

(Associate Professor Anongnat Somwangthanaroj, Ph.D.)

.....Thesis Co-Advisor

(Assistant Professor Wanchai Lerdwijitjarud, Ph.D.)

.....Examiner

(Associate Professor Muenduen Phisalaphong, Ph.D.)

.....External Examiner

(Assistant Professor Suttinun Phongtamrug, Ph.D.)

หนึ่งฤทัย ใจตรง : สมบัติของฟิล์มเป่าพอลิแลคติกเอซิดผสมยางธรรมชาติและเทอร์โมพลาสติกสตาร์ช. (PROPERTIES OF POLY(LACTIC ACID)/NATURAL RUBBER/THERMOPLASTIC STARCH BLOWN FILMS) อ.ที่ปรึกษาวิทยานิพนธ์หลัก: รศ. ดร. อนงค์นาฏ สมหวังธนโรจน์, อ.ที่ปรึกษาวิทยานิพนธ์ร่วม: ผศ. ดร. วันชัย เลิศวิจิตรจรัส, 114 หน้า.

เพื่อศึกษาการปรับปรุงสมบัติของฟิล์มเป่า ฟิล์มเป่าผสมสองและสามองค์ประกอบจึงได้รับความสนใจในงานวิจัยนี้ โดยการผสมระหว่างพอลิแลคติกเอซิด (PLA) กับยางธรรมชาติ (NR) และเทอร์โมพลาสติกสตาร์ช (TPS) ที่อัตราส่วนต่างๆ พอลิเมอร์ผสมนั้นถูกเตรียมขึ้นด้วยเครื่องอัดรีดเกลียวหนอนคู่และขึ้นรูปเป็นฟิล์ม โดยสมบัติเชิงความร้อนและเชิงกล สัณฐานวิทยา การซึมผ่านแก๊ส และการดูดซับไอน้ำของฟิล์มผสมทั้งหมดได้รับการศึกษา จากผลการทดสอบด้วยเทคนิค DSC พบว่า โดเมนยางธรรมชาติใน PLA ซึ่งประพฤติตัวเป็นสารก่อผลึก สามารถเพิ่มระดับความเป็นผลึกของฟิล์มเป่า PLA/NR การเติมยางธรรมชาติลงในฟิล์มเป่าผสมสององค์ประกอบยังช่วยการปรับปรุงความเหนียวและความสามารถในการซึมผ่านแก๊ส ผลการทดสอบแสดงให้เห็นว่า PLA ผสมกับยางธรรมชาติในปริมาณร้อยละ 10 โดยน้ำหนัก เป็นสัดส่วนที่เหมาะสมสำหรับฟิล์มเป่า PLA/NR นอกจากนี้ TPS ยังถูกเตรียมขึ้นโดยการผสมแป้งมันสำปะหลังและกลีเซอรอลในอัตราส่วน 70/30 โดยน้ำหนัก ด้วยเครื่องอัดรีดเกลียวหนอนคู่ ซึ่งการเติม TPS ที่มีสมบัติชอบน้ำลงในระบบส่งผลต่อการเพิ่มขึ้นของความสามารถในการซึมผ่านไอน้ำและความสามารถในการดูดซับไอน้ำของฟิล์มเป่าผสมเป็นอย่างมากโดยเฉพาะอย่างยิ่งที่ปริมาณการเติม TPS สูง ซึ่งเหตุผลที่นำไปสู่ผลลัพธ์เหล่านี้ได้ถูกอภิปรายอย่างถี่ถ้วน ดังนั้น ฟิล์มเป่าผสมสามองค์ประกอบที่ได้จากการผสมระหว่าง PLA กับ NR และ TPS เป็นอีกทางเลือกหนึ่งที่น่าสนใจมากเพื่อพัฒนาสมบัติของฟิล์มบรรจุภัณฑ์ที่ใช้สำหรับยืดอายุพืชผลสด ทั้งนี้ฟิล์มเป่าผสมสามองค์ประกอบนี้ยังผลิตจากวัสดุชีวภาพซึ่งสามารถย่อยสลายได้ง่ายในสภาวะแวดล้อมที่เหมาะสมอีกด้วย

ภาควิชา วิศวกรรมเคมี	ลายมือชื่อนิสิต .....
สาขาวิชา วิศวกรรมเคมี	ลายมือชื่อ อ.ที่ปรึกษาวิทยานิพนธ์หลัก .....
ปีการศึกษา 2556	ลายมือชื่อ อ.ที่ปรึกษาวิทยานิพนธ์ร่วม .....

5670480021 : MAJOR CHEMICAL ENGINEERING
KEYWORDS: THERMOPLASTIC STARCH (TPS) / NATURAL RUBBER (NR) / BLOWN FILM / POLY (LACTIC ACID) (PLA)

NUENGRUTHAI JAITRONG: PROPERTIES OF POLY(LACTIC ACID)/NATURAL RUBBER/THERMOPLASTIC STARCH BLOWN FILMS. ADVISOR: ASSOC. PROF. ANONGNAT SOMWANGTHANAROJ, Ph.D., CO-ADVISOR: ASST. PROF. WANCHAI LERDWIJITJARUD, Ph.D., 114 pp.

In order to investigate the property enhancement, binary and ternary blend films were conducted in this research by blending poly(lactic acid) (PLA) with natural rubber (NR) and thermoplastic starch (TPS) at different contents. PLA-based blends were produced using a twin screw extruder and formed into blown films. Thermal and mechanical properties, morphology, gas permeability and moisture absorption of all samples were evaluated in detail. From DSC results, NR domains in PLA matrix acting as nucleating agent provided high crystallinity percentage in PLA/NR films. Blinding NR in binary blend films provided the improvement of toughness and gas permeability. The results show that PLA blended with 10 wt% of NR was the optimal composition in PLA/NR films. Additionally, TPS was prepared from mixing cassava starch and glycerol at the weight ratio of 70/30 in a twin screw extruder. The incorporation of hydrophilic TPS into the system importantly affected the enhancement of water vapor permeability and moisture absorption of blend films, especially at high TPS loading. The reasons leading to these outcomes were intensively discussed. Consequently, the ternary blend film with the combination of PLA, NR and TPS is a fascinating approach to develop the properties of film packaging used for extending shelf life of fresh produces. This ternary blend film was practically made from bio-based materials which it can easily degrade in the proper environment as well.

Department:	Chemical Engineering	Student's Signature .....
Field of Study:	Chemical Engineering	Advisor's Signature .....
Academic Year:	2013	Co-Advisor's Signature .....

ACKNOWLEDGEMENTS

I would like to express my sincere thanks to my thesis advisor, Associate Professor Dr. Anongnat Somwangthanaroj and my co-advisor, Assistant Professor Dr. Wanchai Lerdwijitjarud for precious advice, guidance and support throughout my research thesis and editing of this thesis.

I am great appreciate to the chairman, Associate Professor Dr. Siriporn Damrongsakkul , and committee members, Associate Professor Dr. Muenduen Phisalaphong and Assistant Professor Dr. Suttinun Phongtamrug who provided significant suggestions and invaluable recommendations for this research.

In addition, I am grateful to everyone in the Polymer Engineering Research Laboratory, Department of Chemical Engineering, Chulalongkorn University, for discussion and friendly encouragement and given comments. Furthermore, I would like to thank my friends, Dr. Uraiwan Pongsa for her kindly helps with editing my thesis and answered my questions all the times.

Finally, I would like to affectionately give all gratitude to the members of my family for their generous encouragement during my entire studies. Also, every person who deserves thanks for the encouragement and support that cannot be listed.

CONTENTS

Page

LIST OF TABLES

Page

LIST OF FIGURES

LIST OF ABBREVIATIONS

BETSE	1,2-bis(triethoxysily)ethane
DSC	Differential Scanning Calorimetry
ENR	Epoxidised natural rubber
HDPE	High density polyethylene
HVA-2	N, N'-m-phenylenebismaleimaide
KNO_3	Potassium Nitrate
LDPE	Low density polyethylene
MD	Machine direction
mPLA	modified Poly(lactic acid)
NR	Natural rubber
OP	Oxygen permeation
OTR	Oxygen transmission rate
PLA	Poly (lactic acid)
PP	Polypropylene
RS	Rice starch
TPS	Thermoplastic starch
T_{cc}	Cold crystallization temperature
TD	Transverse direction
T_m	Melting temperature
T_g	Glass transition temperature

WVP	Water vapor permeation
WVTR	Water vapor transmission rate
X_c	The degree of crystallinity
X_{cc}	The degree of crystallization during heating
X_m	The degree of crystallization during melting
ΔH_m	The specific melting enthalpy
ΔH_{cc}	The specific cold crystallization enthalpy
ΔH_0	The melting enthalpy of 100 % crystalline of PLA

Chapter I

INTRODUCTION

1.1 General Introduction

Recently, there has been growing interest in environmentally friendly bioplastics which are an alternative to petroleum-based plastics. Poly(lactic acid) (PLA) has gained much attention in enormous industrial applications, especially green packaging for fresh produces. PLA has high mechanical properties and excellent transparency; however, it has inherent brittleness which limits its usefulness [1]. Therefore, blending PLA with some elastic material has been received more attention. Natural rubber (NR) is commonly used as a second phase polymer to enhance the toughness of brittle polymers [1, 2]. Many studies have focused on the improvement of mechanical properties of material blended with NR [1-3]. However, little literature is available on the effect of NR content on the properties of PLA blown film for fresh produce packaging.

Proper management of fresh produces prior to packaging and the process during distribution are very important factor to keep the produces fresh. The fresh - cut produces are still living and still require oxygen for their metabolism, the atmosphere inner package should control matching to the gas requirement of the produces. Moreover, the cumulative moisture from the respiration of the produces can easily damage them because it can be used for microbial growth and available for chemical reactions [4]. Accordingly, much attention has focused on blending PLA with the alternative materials to increase gas permeability and water vapor

absorption. Blending PLA with starch, which is an inexpensive renewable biodegradable material, has been extensively studied in recent years [5]. Starch has been frequently processed as thermoplastics for achieving the processability. From the literatures, it was found that blending starch achieved high gas permeability and water absorption of resultant film because starch is very sensitive to moisture content [6-8]. Consequently, blending PLA/NR with TPS is an interesting approach.

This study is designed to evaluate the effect of binary blends on the properties of PLA-based blown films. Blending PLA with different NR and TPS contents was considered. Moreover, the ternary blend films were produced by blending PLA/NR10 with various TPS loading. Thermal properties, morphology and moisture absorption of blend films were evaluated. Gas permeability was investigated in term of oxygen and water vapor transmission rate. Mechanical properties of blown films were elucidated as well.

1.2 Objectives

To study the effect of the presence of NR and TPS in binary and ternary blends on the different properties of PLA-based blown films

1.3 Scopes of the research

1.3.1 Investigate the effect of binary blends between PLA and various NR contents in blown films

1.3.2 Evaluate the effect of binary blends between PLA and different TPS loading in blown films

1.3.3 Examine the effect of ternary blends between PLA/NR and varied TPS contents in blown films

Chapter II

THEORY AND LITERATURE REVIEWS

This chapter describes the general information of Poly(lactic acid), natural rubber, thermoplastic starch and the gas permeation mechanism. In the first part, the effect of PLA/NR/TPS blended will be explained. In the second part, the gas permeation mechanism of film and the related factor will be discussed.

2.1 Biodegradable plastic

A growing rate of production of materials, products, and manufacturing is increasing steadily. Bioplastic has played an important role in global production as shown in Figure 2.1[9].

Figure 2.1 Global production capacities of bioplastics [9]

2.1.1 Poly(lactic acid) (PLA) and Natural rubber (NR)

Poly(lactic acid) (PLA) is polyester derived from the polymerization of a renewable resources such as corn and cassava. PLA is a popular biodegradable plastic to use as packaging films. Natural rubber (NR) as an elastic material is commonly used as a second phase polymer for the toughness enhancement of PLA. Many studies have focused on the mechanical properties of PLA/NR blend. It was found that the addition of NR in PLA matrix provided ductile material as shown in Figure 2.2. From the stress-stain curve of PLA/NR blend, the necking and cold drawing could be observed during stretching of specimens [2].

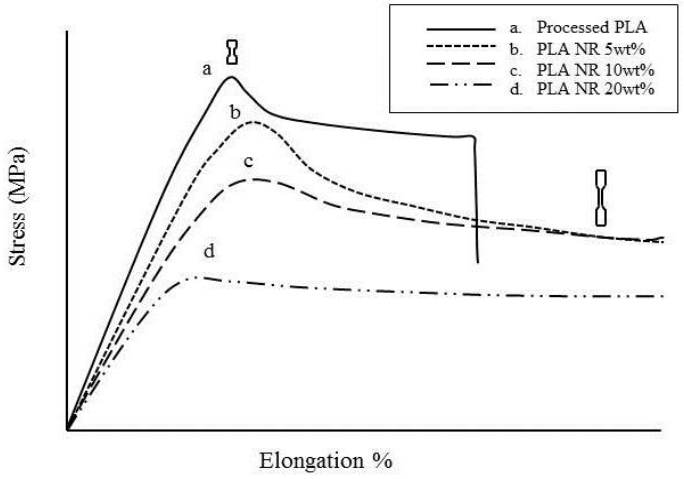

Figure 2.2 Stress-strain curve of PLA/NR blends [2]

Adding 10 wt% NR enhanced the elongation at break from 5 % of neat PLA to 200 %. However, tensile strength decreased from 63.1 MPa for neat PLA to 50.4, 40.1 and 24.9 MPa for PLA blended with NR at 5, 10 and 20 wt%, respectively [2]. The addition of NR latex in PLA matrix exhibited an increase in the elongation at break from 10 to 21.5 %. Also, the tensile toughness was enhanced from 330 MPa for

neat PLA to 735 MPa for PLA/10 wt% NR [10]. The incorporation of NR improved the elongation at break and the tensile toughness but decreased impact and tear properties of PLA/NR when compared with neat PLA [11].

NR domains act as a stress concentrator which lead to crazes, cracks and propagates during the fracture process. The formation of stress whitening can be observed in film because of the effect of light scattering as shown in Figure 2.3. Crazing induced energy dissipation in the PLA matrix which retarded crack initiation and propagation and led to an improved toughness for the brittle PLA [12, 13].

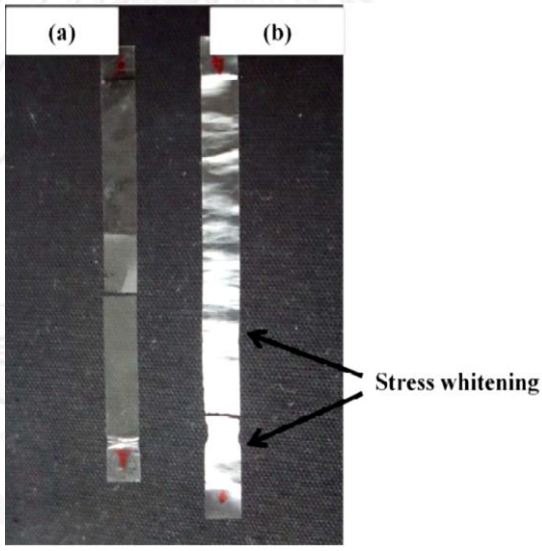

Figure 2.3 Crazing of PLA/NR film a) neat PLA film b) PLA/NR film

The morphology of PLA/NR film is illustrated in Figure 2.4. PLA matrix was the continuous phase and NR was the dispersed phase. Because PLA and NR are immiscible blend, it was observed that the cavities were left by NR domains in cross sectional image. Moreover, the coalescence of rubber domain was occurred as increasing of NR content [11].

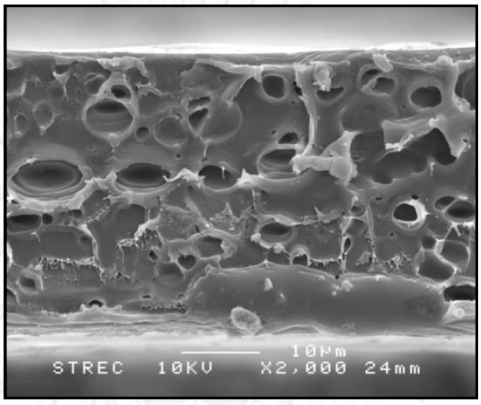

Figure 2.4 SEM micrograph of PLA/10 wt% NR blown film in MD direction [11]

2.1.2 Poly(lactic acid) and Thermoplastic starch (TPS)

Starch is a compostable and renewable polymer which is extracted from plants such as wheat, corn, potato, rice and cassava. Commonly, the starch has a hydrophilic character. The starch is mainly composed of amylose and amylopectin. Amylose is a linear chain of glucose monomer which is bonded by α (1-4) bond, and amylopectin is a branch chain of glucose which is formed by α (1-4) bond in linear and 1-6 linkage in branching. Figure 2.5 illustrates the structure of amylose and amylopectin in starch granule [14].

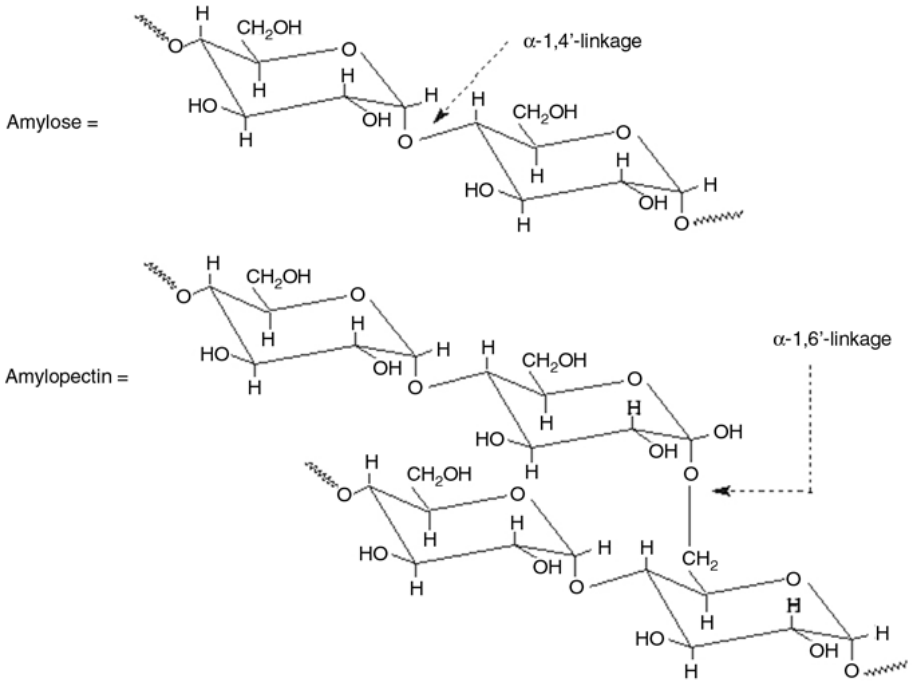

Figure 2.5 Amylose and amylopectin structure [12]

Starch is usually composed of hydrogen, carbon and oxygen; however, it has some impurity such as protein, lipid and minerals. Starch with high content of impurities especially protein is called “flour” such as corn flour, wheat flour, rice

flour. These impurities in starch are obstructed the plasticization process. On the other hand, high purity starch can be obtained from potato and cassava [15].

The granule of starch has very strong hydrogen bond. Therefore, the glass transition temperature (T_g) and the melting temperature (T_m) are higher than the degradation temperature (T_d). To reduce T_g and T_m for extrusion process, adding plasticizer into starch can be performed. Glycerol is an alternative plasticizer because it is a small molecule and can easily move into starch granule. While starch absorbs glycerol under the heating and shearing, hydrogen bonds between hydroxyl groups of starch is broken. Then, the starch granule is destroyed, plasticized and melted (Figure 2.6). After the processing, it is become a melted and partially depolymerized starch which is referred to as thermoplastic starch “TPS” [14].

The plasticization process is called “gelatinization” process. The starch granule is highest swollen by plasticizer at the gelatinization temperature. Figure 2.7 shows the gelatinization process.

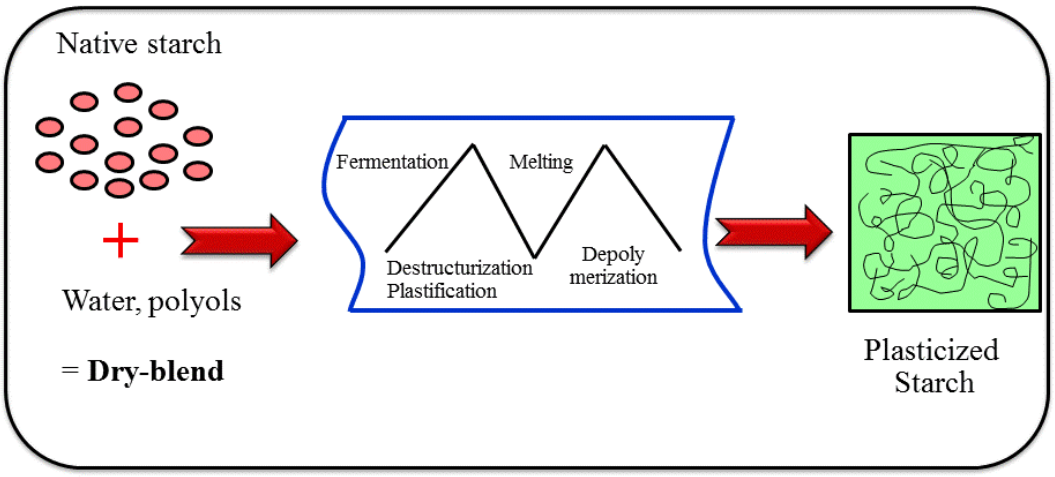

Figure 2.6 Thermoplastic starch process by extrusion [12]

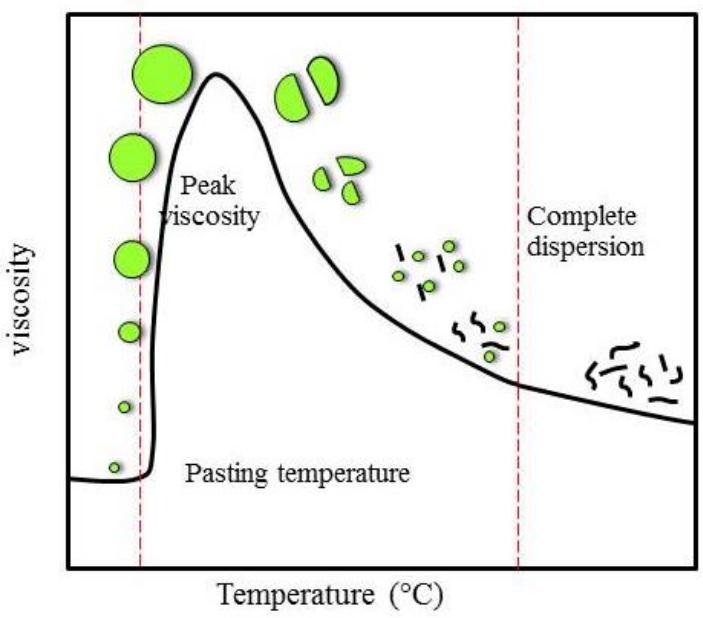

Figure 2.7 Gelatinization process [13]

Cassava starch is an important economic crop of Thailand. It has less impurity and is easy to handle for plasticization. The impurity composition of cassava starch compared with that of rice flour is shown in Table 2.1[15].

Table 2.1 Composition of impurities in starch and flour [13]

Impurity	Cassava starch	Rice flour
Moisture (65% RH, 20 °c)	13	N/A
% Lipid	0.1	0.8
% Protein	0.1	0.45
% Phosphorus	0.01	0.1

Many research studied about blending starch with other thermoplastics to reduce cost and petroleum-based plastic waste problem. Most of synthesized polymer is a hydrophobic material. Blending of starch and other biopolymers provided an immiscible blend. Figure 2.8 reveals a two-phase morphology of corn starch/low density polyethylene (LDPE) blown film. LDPE was the continuous phase and starch was the dispersed phase. LDPE/starch film exhibited micro voids with an increase of starch contents [6].

Mechanical properties of starch blends were dropped. Tensile strength and elongation at break of films decreased with increasing of starch content. The

tensile strength in MD of LDPE (19.8 MPa) decreased to 8.9 MPa with the addition of 50 wt% starch into blown film. This is due to incompatibility of starch and LDPE [6].

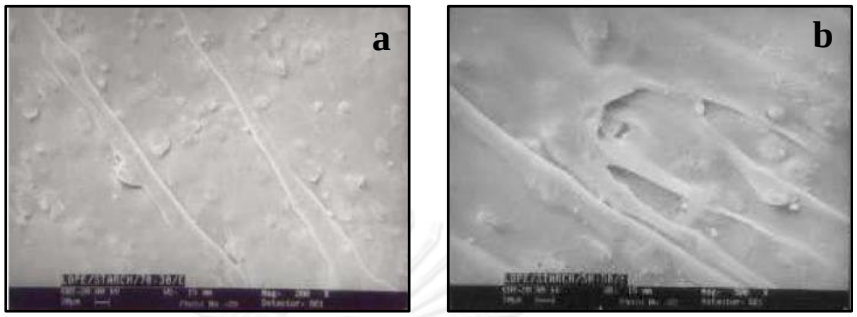

Figure 2.8 SEM micrographs of LDPE/starch blown film a) LDPE/starch (70/30) and b) LDPE/starch (50/50) [7]

In addition, the impact strength of LDPE/starch blown film decreased from 17.1 g for pure LDPE to 0.6 g for 50 wt% starch film [6]. The tear strength, which is an important property of films, of LDPE/starch films decreased with increasing of starch content. Decreasing of tear strength may be due to the immiscibility of starch in continuous LDPE matrix [6, 8]

Moreover, some research was investigated about 3 phases of polymer blends. Incorporation of epoxidised natural rubber (ENR50) in PLA/rice starch (RS) blend improved the tensile strength and elongation at break. It is mainly because the addition of ENR50 enhanced the interfacial interaction between PLA matrix and RS particles. Figure 2.9 illustrates the fracture surface of PLA/RS and PLA/RS/ENR50 composites. For PLA/RS/ENR50, the gap between PLA and RS particles was smaller and closer than that of PLA/RS. This indicated that the wettability of the RS by PLA matrix had been improved [3]. In addition, blending of high density polyethylene (HDPE), NR and TPS was studied into 2 series i.e. unvulcanized and *N, N'-m-*

phenylenebismaleimide (HVA-2) vulcanized. Tensile strength, Young's modulus and elongation at break of both series decreased because of the poor interfacial adhesion of TPS and HDPE/NR matrix. However, the mechanical properties of vulcanized HDPE/NR/TPS were found to increase comparing with those of unvulcanized HDPE/NR/TPS. This is due to the fact that HVA-2 (crosslink agent) could promote the intra- and intermolecular linkages in NR phase, resulting in the improvement of blend's properties [16].

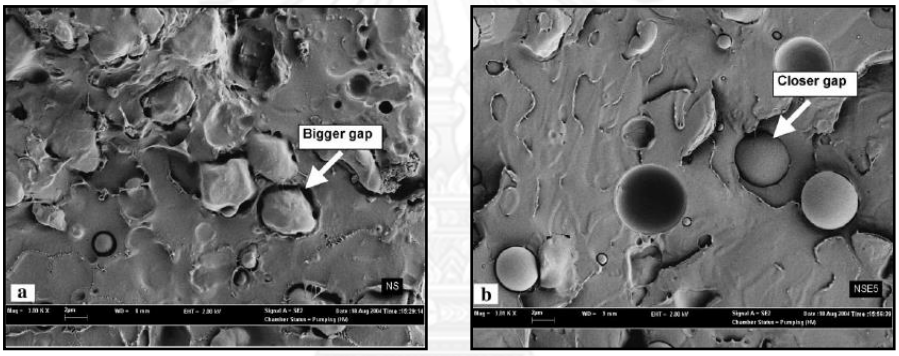

Figure 2.9 SEM micrographs taken from the cryogenic-fractured surface of (a) PLA/RS20 and (b) PLA/RS20/E5 [3]

2.2 Permeation mechanism

The potential packaging films should have high gas permeability that can absorb gas occurred in the package by the respiration of fresh produces and then diffuse them to surrounding environment. The film with high gas permeability is strongly required to prolong the shelf life of fresh produces having high rate of respiration. For the permeation mechanism in which pressure is a driving force, there are 3 mechanisms including absorption, diffusion and desorption. The permeability of film is a function of film's properties, the nature of gas species and interaction between

film and gas. The properties of film and the nature of gas species refers to the sorptivity or solubility of gas in films, while the interaction between film and gas refers to the gas diffusion in film [17].

2.2.1 Properties of film

Gas permeation in film is affected by properties of film such as degree of crystallinity, free volume and composition of filler. The presence of crystalline structure in films can result in lower oxygen permeation. The crystal may obstruct O_2 passing through the film. Moreover, the larger sized crystals provide the brittleness of the structure leading to voids in the film. From literature, the O_2 permeation (OP) of polypropylene (PP) compounded at 190 °C and molded by different cooling rate was investigated [18]. It was found that the OP increased from 2,660 cc.mil/(m^2.day.atm) for fast cooling to 2,929 cc.mil/(m^2.day.atm) for slow cooling because of defects at boundaries of larger sized crystals.

The free volume is a space in polymer that is not occupied by polymer molecules as shown in Figure 2.10 [19]. Amorphous polymers may have high free volume compared with semi-crystalline polymer. Polymer chains of amorphous materials can easily move and create high free volume fraction. The permeability (P) of LDPE (5.10×10^{13} cc-mil/(m^2.day.atm)) is lower than that of NR (2.60×10^{14} cc-mil/(m^2.day.atm)) [20].

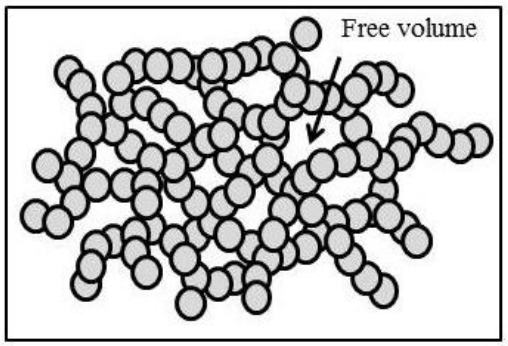

Figure 2.10 Free volume in polymer [17]

For noncontinuous polymeric materials, gas permeation can pass through not only the matrix and domain parts but also the interfacial part. The OP and water vapor permeation (WVP) of PLA/NR and PLA/maleated natural rubber (MNR) films increased with increasing of NR and MNR contents, respectively. Moreover, adding 2.5 wt% fume silica into PLA/MNR blends enhanced the OP from 792 cc.mil/m^2.day.atm for pure PLA film to 11,276 cc.mil/m^2.day.atm for PLA/MNR/fume silica film [11]. The WVP of PLA/MNR also increased from 189 gm mil/m^2.day.atm for pure PLA film to 289 gm mil/m^2.day.atm for PLA/MNR/fume silica one.

2.2.2 The properties of gas species

Size and polarity of gas species remarkably affect the solubility. The smaller sized gas can easily pass through the film. Kinetic parameter of gas species is shown in Table 2.2. The permeation of H_2 in 1,2-bis(triethoxysilyl)ethane (BETSE) membrane is higher than that of CO_2 and N_2, respectively. This permeation depends on kinetic diameter of gas molecule [21]. Moreover, the polarity of gas is also involved with the interaction between gas and film. The polarity of gas is displayed

by the dipole moment as shown in Table 2.2. The polar gas has strong interaction between gas and polar film.

Table 2.2 kinetic diameter and dipole moment of gas species

Gas molecules	Kinetic diameter (A°)	Dipole moment
CH_4	3.80	0
N_2	3.64	0
O_2	3.46	0
CO_2	3.30	0
H_2	2.89	0
H_2O	2.65	1.84
He_2	2.60	0

2.2.3 The interaction between gas and film

As mentioned previously, the polarity of film was intensely important to obtain interaction between gas and film. The polar of film can evaluate by measuring the contact angle of water drop on film. Contact angle is the angle between liquid and surface of film which indicates the degree of wetting. The high contact angle (> 90°) is referred to low wettability, while small contact angle (<90°) is referred to high wettability [22]. Pure PLA and modified PLA (mPLA) films have smaller water contact angle than LDPE films, resulting in higher water vapor wettability [23].

Table 2.3 Water contact angle of films [21]

Films	Water contact angle (°)	WVP (g/m^2-day)
PLA	77.1	166.02 ± 0.16
mPLA	79.3	137.37 ± 1.13
LDPE	92.5	7.26 ± 0.57

In addition, PLA/RS composite has higher moisture absorption and diffusion constant than neat PLA about 5 and 1.24 times, respectively. This is due to the presence of the hydroxyl groups in starch granule which could interact with water molecules. Moreover, moisture absorption and diffusion constant slightly increased with the addition of ENR50. This might be due to the water molecule passing through the interfacial zone (PLA/RS and PLA-ENR) [3].

CHAPTER III

EXPERIMENTS

3.1 Materials

PLA grade 2003D was obtained from NatureWorks®, USA. Air-dried sheet natural rubber (NR) was brought from Hi Karn Yang, Rayong, Thailand. Cassava starch with 13% of moisture (New grade) was purchased from Thai wah food products, Thailand. Analytical grade glycerol used as plasticizer was purchased from Qrec, New Zealand. Potassium Nitrate (KNO_3) was supplied by Rankem, India.

3.2 Preparation of PLA/NR blown films

Blending of PLA and NR was carried out by using a co-rotating twin screw extruder with L/D = 40, D = 20 mm (Lab Tech, Thailand). The composition of PLA/NR was tabulated in Table 3.1. The processing temperature was 185-190°C. The screw speed was 80 rpm. The extrudate was cut into 2.5 mm of length. Finally, the PLA/NR pellets were dried in an oven at 60°C overnight and stored in PE zipped-lock plastic bag before they were extruded into films.

The PLA/NR blown films were produced in a single screw extruder with L/D = 25, D = 20 mm attached to blown film line (Collin, Blown film line BL 180/400E, Germany). The processing temperature is 190-196°C. The screw speed was 85 rpm. The speed of the nip roll was adjusted to produce a film with a thickness of 40 μm.

3.3 Preparation of PLA/NR/TPS blown films

Cassava starch was ground and dried in an oven at 75°C overnight. After that, Cassava starch was premixed with 30 wt% of glycerol by hand mixing and then the mixture is stored overnight. Next, the mixture was extruded using a co-rotating twin screw extruder with L/D = 40, D = 20 mm (Lab Tech, Thailand). The processing temperature was 80-135 ºC and the screw speed was 45 rpm. After that the obtained extrudate TPS was cut into 2.5 mm of length. Finally, the pelletized TPS was dried in an oven at 50°C overnight and stored in PE zipped-lock plastic bag.

The composition of PLA/NR/TPS was shown in Table 3.1. The preparation method was similar to the preparation of PLA/NR blends as mentioned above. For blending process, the temperature of extruder was 175-190° C and the screw speed was 80 rpm. For blown film process, the temperature of extruder was 180-185°C and the screw speed was 85 rpm.

Table 3.1 Composition of blends

Sample	Blend composition (wt%)		
	PLA	NR	TPS
PLA	100	-	-
PLA/NR 5	95	5	-
PLA/NR 10	90	10	-
PLA/NR 15	85	15	-
PLA/NR 10/TPS 5	85	10	5
PLA/NR 10/TPS 10	80	10	10
PLA/NR 10/TPS 15	75	10	15

3.4 Characterization

3.4.1 Thermal properties

The thermal properties of blown films were examined by using a differential scanning calorimeter (DSC; TA Instruments 2910, USA). Samples of 5-10 mg in an aluminum pan were heated from 30 to 200 °C at a heating rate of 10 °C/min. The glass transition temperature (T_g), cold crystallization temperature (T_{cc}) and melting temperatures (T_m) were obtained from DSC curve. The degree of crystallinity (X_c) of samples was calculated by the following equation.

$$X_c = \frac{\Delta H_m - \Delta H_{cc}}{\Delta H_0 \times \Phi_{PLA}} \times 100$$

where ΔH_m and ΔH_{cc} are the enthalpies of the melting and cold crystallization of samples, respectively. Φ_{PLA} is the weight fraction of PLA in the blends and ΔH_0 (93.6 J/g) is the melting enthalpy of 100 % crystalline of PLA [24].

3.4.2 Morphology

The cross section of blown films in machine direction (MD) and transverse direction (TD) were observed by using scanning electron microscope (SEM, JEOL JSM 5800LV, Japan) at an acceleration voltage of 15 kV. The blown films were cut under liquid nitrogen and fixed on stubs and then coated with gold prior to SEM observation. The PLA/NR films were strained with osmium tetroxide vapor before coating with gold because the phase contrast between PLA matrix and NR domain was shown.

3.4.3 Permeability properties

The oxygen transmission rate (OTR) of blown films was examined according to ASTM D 3985 by using oxygen permeability analyzer (Mocon OX-TRAN model 2/21) with oxygen flow rate of 40 cm^3/min at 23 ℃ and 90% of relative humidity.

The water vapor transmission rate (WVTR) of blown films was measured according to ASTM E 398 using water vapor permeability analyzer (Mocon PERMATRAN-W model 398) with nitrogen flow rate of 250 cm^3/min at 37.8 ℃ and 90% of relative humidity.

3.4.4 Moisture absorption

Moisture absorption rate was carried out in a box with controlled at 90 % of relative humidity. The relative humidity was controlled by the saturated KNO_3 solution. All films were dried until constant weight and weighted before and after absorption times. The moisture absorption value was calculated by the following equation.

$$M_t\% = \frac{M_t - M_0}{M_0} \times 100$$

where M_t is the mass of film at a time t and M_0 is the initial mass of film [25].

3.4.5 Water contact angle

The wettability of films was evaluated by measuring the contact angle of water drop on film by using Tantec CAM v3.08 software. Water was dropped on film surface and captured by camera. The program calculated the contact angle values.

3.4.6 Mechanical properties

The impact resistance of blown films was investigated according to ASTM D 3420 by using film impact testing machine (Digital impact tester, Toyoseiki, Japan). The specimens were prepared in dimension of 10 x 10 cm.

The tear strength of blown films was evaluated according to ISO 6383 by using tear testing machine (Digital Elmendorf type tearing tester model SA, SA-W, Toyoseiki, Japan). The specimens were prepared in dimension of 6.3 x 7.3 cm.

The tensile strength, young's modulus, and elongation at break of blown films were studied according to ASTM D 882 by using universal testing machine (Instron: model 5567, USA). The crosshead speed used in this work was 12.5 mm/min at 1 kN of load cell. Measurements were conducted in both machine and transverse directions. Ten specimens were tested for each formulation and each direction.

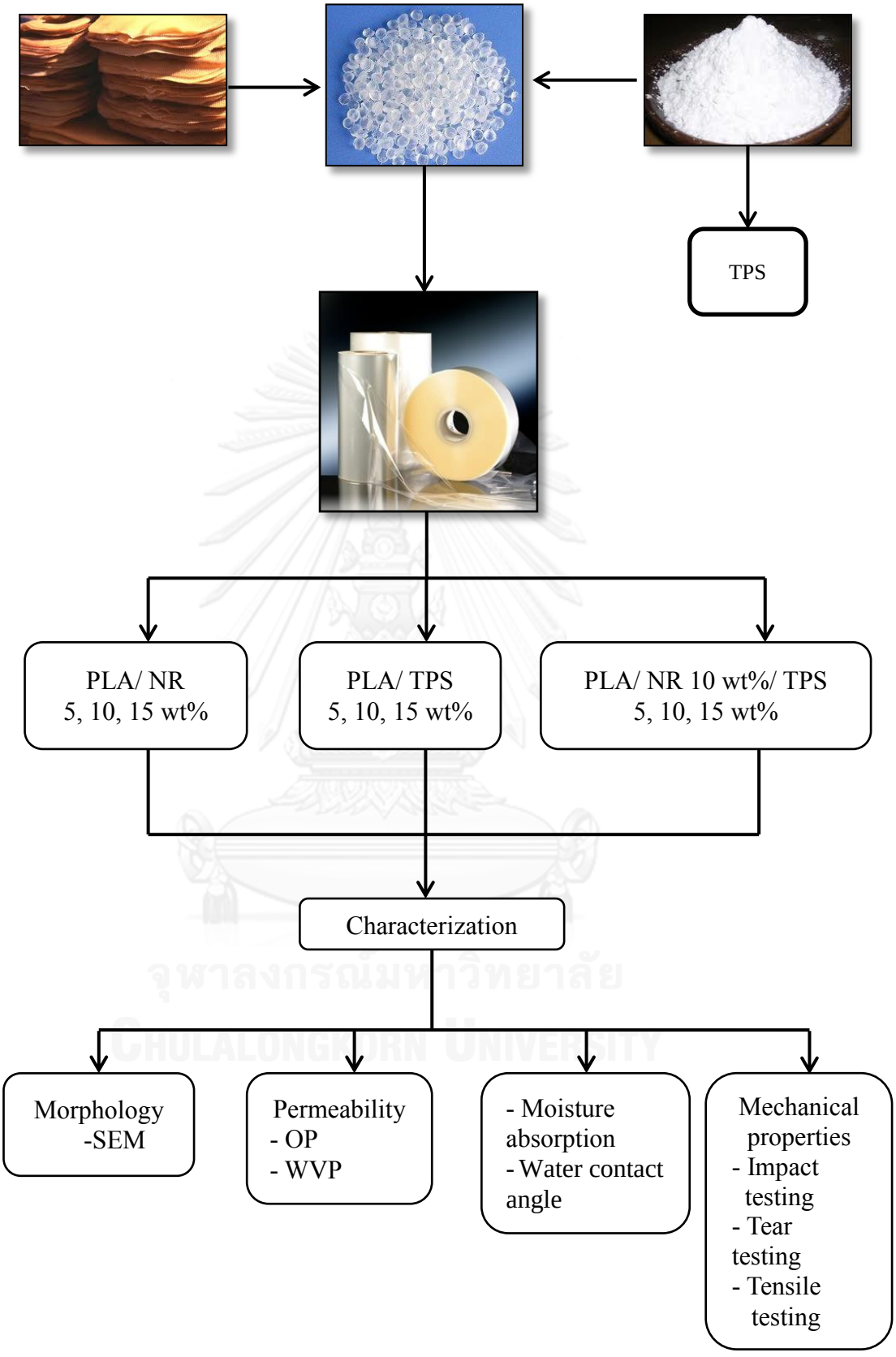

Figure 3.1 The experiment procedure

CHAPTER IV

RESULTS AND DISCUSSIONS

This study aims to achieve the properties of PLA blown films by melt blending with natural rubber (NR) and thermoplastic starch (TPS). The experiments were designed to study the effect of the binary and ternary blends on their properties. The thermal properties, surface properties and permeability of films were investigated. The mechanical properties of films were also elucidated because these can quantify how much stress the films can stand before suffering permanent deformation. Tensile properties, impact and tear resistance of films were also evaluated as well.

4.1 Binary blend films of PLA and NR

Air dry sheet NR was cut into small pieces and then blended with PLA at 5, 10, 15 wt% in a twin screw extruder. The binary blend films were blown with a thickness of 40 μm. The properties of resultant films were characterized and discussed as follows

4.1.1 Thermal properties

DSC thermograms of neat PLA and PLA/NR blend films in the first heating are presented in Figure 4.1. It is clearly observed that the values of glass transition temperature (T_g) of binary blend films were close to that of neat PLA film approximately ~59 °C. This is suggested that blending NR did not affect the T_g of binary blend films, resulting in the characteristic of immiscible blend [2, 26, 27].

It is obviously seen that the exothermic peak of cold crystallization temperature (T_{cc}) of neat PLA was very broad, whereas the narrow peaks were observed for blend films. The T_{cc} peaks shifted to lower temperature with increase in NR content. The T_{cc} decreased from ~122 °C for neat PLA film to ~102 °C for PLA film blended with 15 wt% NR. These behaviors imply that blending NR induced a faster crystallization because NR acted as a nucleating agent [2]. The specific cold crystallization enthalpy (ΔH_{cc}) directly determined from the area of T_{cc} peak gradually decreased as NR loading increased, referring to the reduction of the degree of crystallization during heating (X_{cc}). It is consistent with the previous studies [10, 28]. The data derived from DSC curves in the first heating is tabulated in Table 4.1.

Considering the endothermic peaks of melting temperature (T_m), the presence of double melting peaks was observed in PLA films blended with NR probably due to melt-recrystallization mechanism of semi-crystalline PLA [29]. The low melting temperature (T_{m1}) could be attributed to the melting of crystals occurring during cold crystallization and the high melting temperature (T_{m2}) was related to the melting of original crystals generating during blown film processing. It is evident that the relative intensity of T_{m1} decreased as NR loading increased because small amounts of crystals were produced during cold crystallization at high NR loading. More interestingly, the degree of crystallization during melting (X_m) in blown films, related to the specific melting enthalpy (ΔH_m), increased with increase in NR content [30]. The specific melting enthalpy (ΔH_m) was directly determined from the area of T_m peak. It might be explained by the fact that blending NR enhanced the crystallization during blown film processing. Mostly, the percentage of crystallization

(X_c) occurring during blown film processing could be calculated as a following equation:

$$X_c = \frac{\Delta H_m - \Delta H_{cc}}{\Delta H_0 \times \Phi_{PLA}} \times 100$$

As expected, the values of X_c increased with the presence of NR which was a nucleating agent for binary blend films.

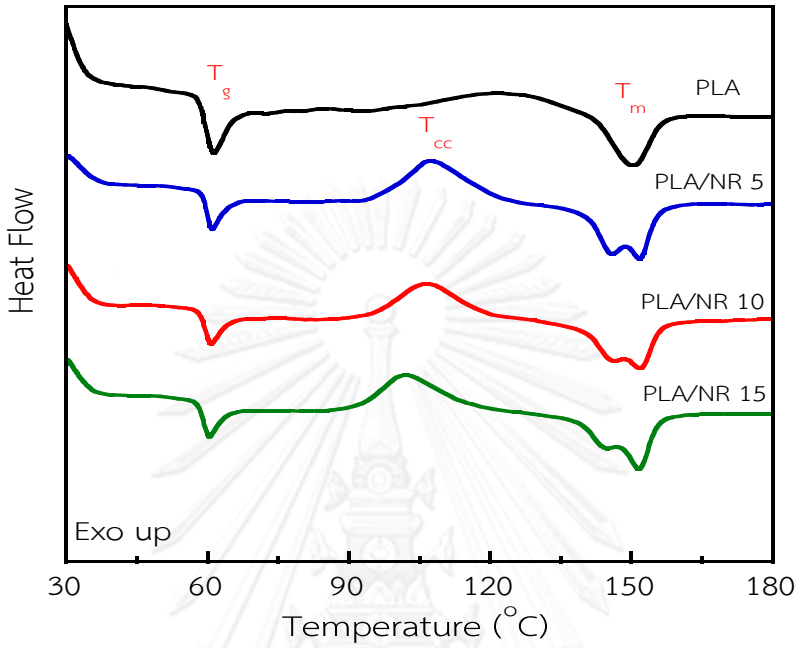

Figure 4.1 DSC thermograms in first heating scan of binary blends PLA/NR films

Table 4.1 DSC data of binary blends PLA/NR films

Sample	T_g	T_{cc}	T_{m1}	T_{m2}	ΔH_m	ΔH_{cc}	X_m	X_{cc}	X_c
PLA	59.5	122.6	-	150.5	14.9	12.3	16.0	13.3	2.7
PLA/NR 5	59.8	107.2	146.0	151.8	24.7	21.2	27.9	24.0	3.9
PLA/NR10	59.2	106.6	146.3	151.8	21.9	17.9	26.1	21.4	4.7
PLA/NR15	59.0	102.1	145.1	151.7	23.5	19.4	29.8	24.5	5.2

Note: ΔH_m - The specific melting enthalpy (J/g)

ΔH_{cc} - The specific cold crystallization enthalpy (J/g)

X_m -The degree of crystallization during melting (%)

X_{cc} - The degree of crystallization during heating (%)

X_c - The degree of crystallinity (%)

4.1.2 Morphology

In order to observe the morphology of NR in PLA matrix clearly, the fracture specimens were stained with osmium tetroxide vapor before SEM experiment. Osmium tetroxide vapor could react with the double bonds of the unsaturated carbon-carbon bonds of NR chains, enhancing phase contrast. The morphology of blown films was investigated both machine direction (MD) and transverse direction (TD). Figure 4.2 illustrates SEM micrographs of fracture of films in MD. It is clearly observed that binary blend films exhibit a phase–separated structure in which NR domains were apparently dispersed in the continuous PLA matrix. Increasing NR contents, the oval cavities or domains were larger probably due to the agglomeration of NR.

As expected, the profile of dispersed NR domains in TD was different from that in MD. More stretched NR domains were evident in fracture surface of films in TD as shown in Figure 4.3. It can be explained by the effect of blow film processing. A film bubble was continuously pulled up by a speed of nip rolls unit in MD and expanded in TD by air blowing. Polymer chains were usually orientated in MD rather than in TD. Accordingly, NR domains were more favorable to expand and stretch along the direction of polymer chain orientation.

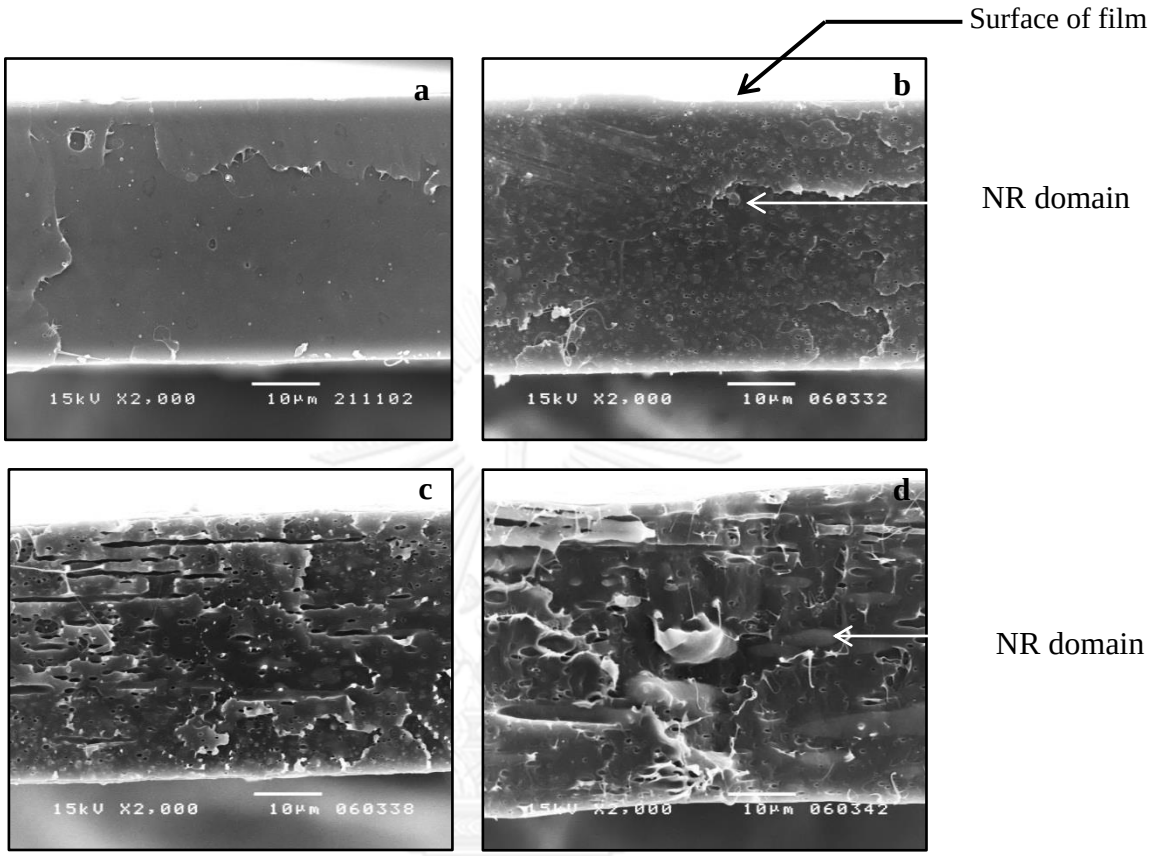

Figure 4.2 SEM micrograph of binary (PLA/NR) blend films in MD

a) Neat PLA, b) PLA/NR5, c) PLA/NR10, d) PLA/NR15

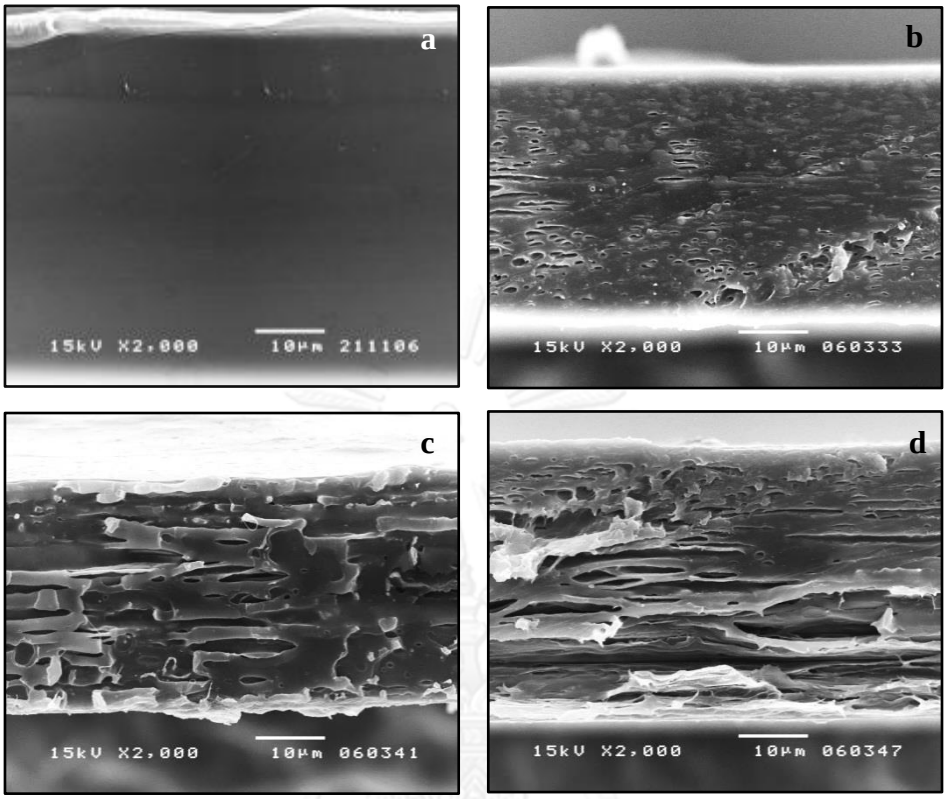

Figure 4.3 SEM micrograph of binary (PLA/NR) blend films in TD

a) Neat PLA, b) PLA/NR5, c) PLA/NR10, d) PLA/NR15

4.1.3 Hydrophobicity and Moisture absorption

In order to investigate the hydrophobic characteristic of resultant films, the contact angle of water droplet on their surfaces was measured. It was found that the values of water contact angle slightly increased with increasing of NR contents as shown in Table 4.2. This is indicated that PLA/NR films have lower water wettability than neat PLA film.

Moisture absorption of samples was also examined as a function of immersion time at 94.73 ± 2.15 %RH and 19.94 ± 1.23 °C. The percentage of moisture absorption was rarely increased with increasing time as demonstrated in Figure 4.4. Interestingly, the absorption rate of blend films was higher than that of neat PLA film. The value of moisture absorption was not over 1 % for all samples because of their hydrophobic characteristic. It is probably due to the absorption of water molecules into the film mainly occurring at the interface between of PLA matrix and NR domain [3]. The variation in the data of moisture absorption was significantly observed. It might be reasoned by the effect of the weighing film process in the open system which some water vapor molecules could evaporate during that period of time.

4.1.4 Gas permeability properties

Water vapor permeation (WVP) and oxygen permeation (OP) of PLA films blended with various contents of NR is depicted in Figure 4.5. The WVP values slightly increased with the increase of NR content. Due to the immiscible blend and low interfacial adhesion between PLA and NR, the gaps were formed at the interface. Besides, draw-back of elastic NR domains after stretching in blow film processing also

caused the large gaps between the phases, indicating high free volume fraction. Mostly, elastic materials show high gas permeability because of high free volume in their structure [17]. When NR content increased, free volume fraction of blown film increased. Consequently, high amounts of water vapor molecules could easily diffuse through the film having high free volume fraction.

In addition, the OTR values remarkably increased 16.46, 31.99 and 40.41 % by blending PLA with NR at 5, 10 and 15 wt%, respectively. The phenomenon of OP is similar to WVP as aforementioned.

Considering PLA film blended with NR 15 wt%, it was found that OP enhanced 40.41 %, whereas WVP only increased 12.40 %. It is associated with the polarity of gases and PLA/NR films. Oxygen (O_2) is non-polar gas which is highly soluble in non-polar films, resulting in higher O_2 adsorption on the surface of films.

Table 4.2 Water contact angle of binary (PLA/NR) blend films

Sample	Water contact angle (°)
Neat PLA	70.76 ± 0.19
PLA/NR 5	70.56 ± 0.28
PLA/NR 10	73.95 ± 0.01
PLA/NR 15	73.41 ± 0.30

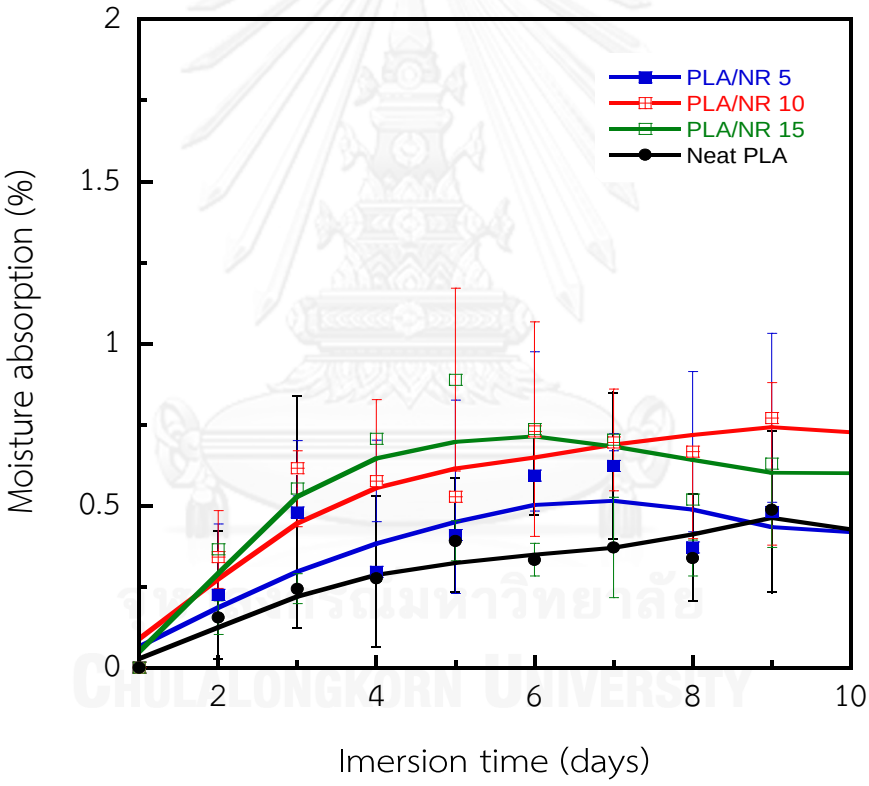

Figure 4.4 Moisture absorption of binary (PLA/NR) blend films

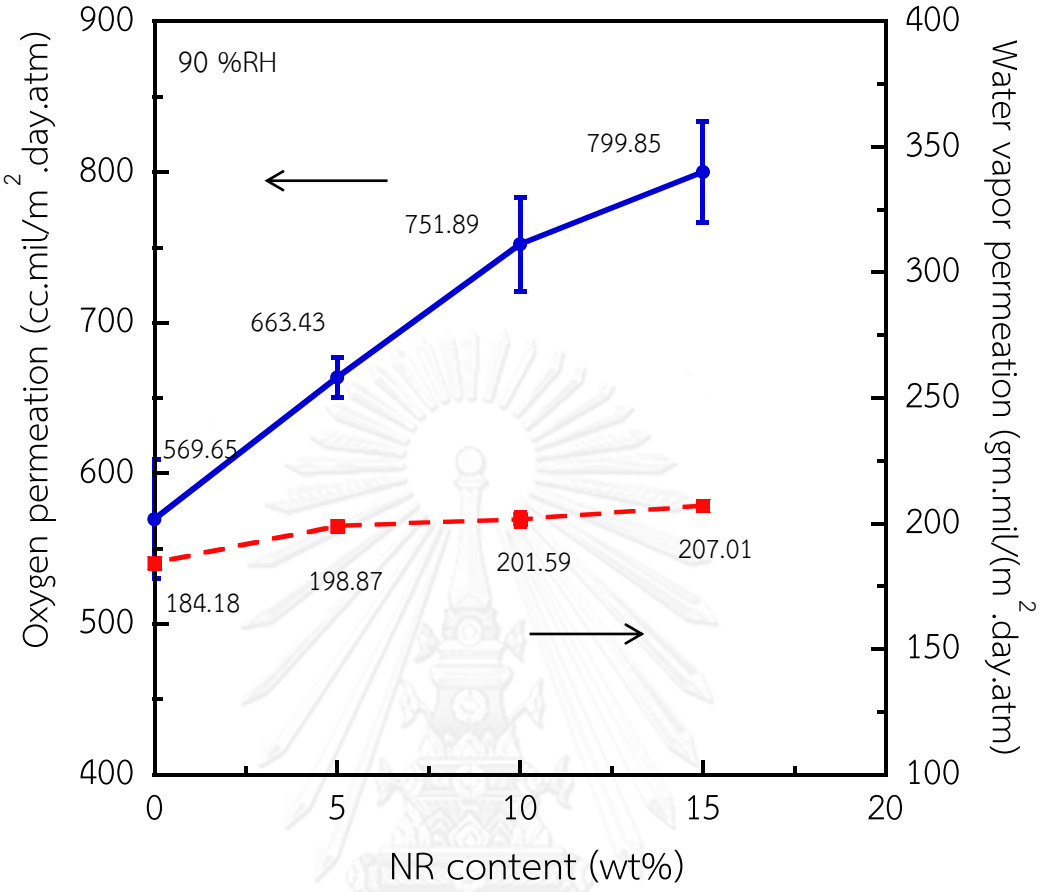

Figure 4.5 Oxygen and water vapor permeation of binary (PLA/NR) blend films

4.1.5 Mechanical properties

The tensile properties of binary blend films could be analyzed from the stress-strain curves as displayed in Figure 4.6. Neat PLA exhibits brittle fracture characteristic with short plastic deformation zone after yield point while PLA/NR films show longer plastic flow region, indicating enhanced toughness. Figure 4.7 demonstrates the photograph of deformed specimens after tensile testing. The corporation of NR led to the decrease of Young's modulus and tensile strength as seen in Figure 4.8.

As shown in Figure 4.9, it is noticeable that the elongation at break and tensile toughness increased with adding NR into PLA matrix. The maximum value was found at 10 wt% NR loading. This result confirms that the toughness of blend films achieved with blending NR [3, 24, 28].

Furthermore, the tear strength of blown films as depicted in Figure 4.10 increased when the concentration of NR increased. Remarkably, the tear strength in TD was higher than that in MD. Tear behavior was highly influenced by the orientation distribution of polymer chains and dispersed domains with respect to the tearing direction. The preferential orientation of PLA chains and stretched NR domains parallel to the MD was responsible for the low tear strength in the MD and the difference between the MD and TD tear strengths of blend films. The possible tear mechanisms were proposed as illustrated in Figure 4.12.

Figure 4.12 shows the impact strength of neat PLA and PLA films blended with different NR content. PLA film blended with 10 wt% NR provided the effective enhancement which the impact strength increased about 6 folds, comparing with neat PLA film. This is due to the fact that the dispersed NR domains could absorb

and dissipate the applied energy to other domains before cracking. When NR content increased, an acceptor of dissipation energy increased [24]. Considering at 15 wt% NR, the impact strength trends to decrease because of the large size NR domain as mentioned above.

From the results in this part, PLA film blended with 10 wt% NR was high efficient system because the toughness and mechanical properties intensely enhanced. Consequently, the concentration of NR at 10 wt% was selected to further use in the section 4.3.

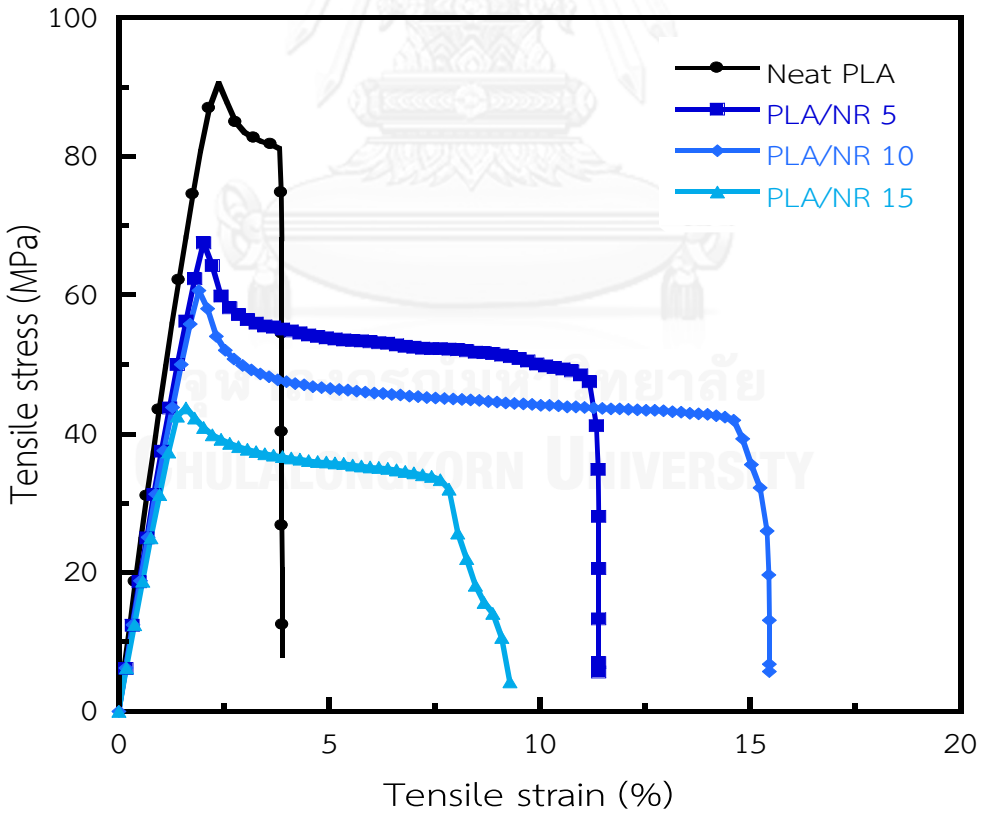

Figure 4.6 Stress strain curve of binary (PLA/NR) blend films

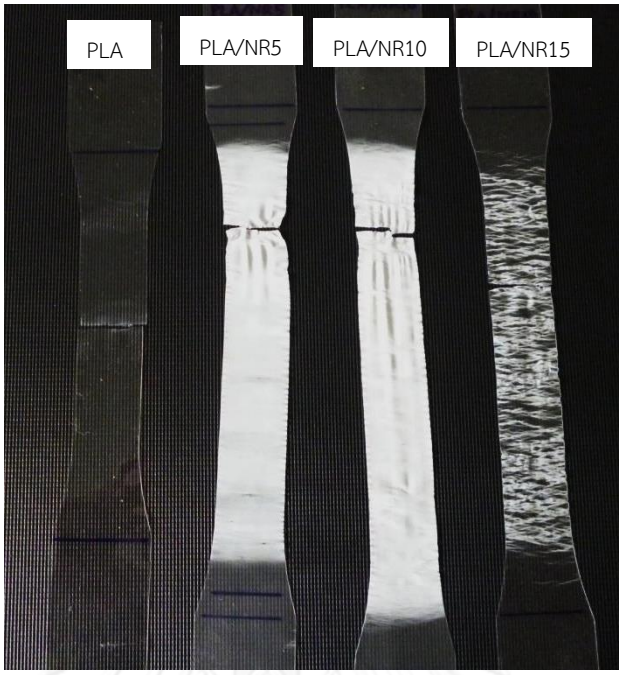

Figure 4.7 The photograph of deformed specimens after tensile testing of neat PLA and PLA/NR blend films

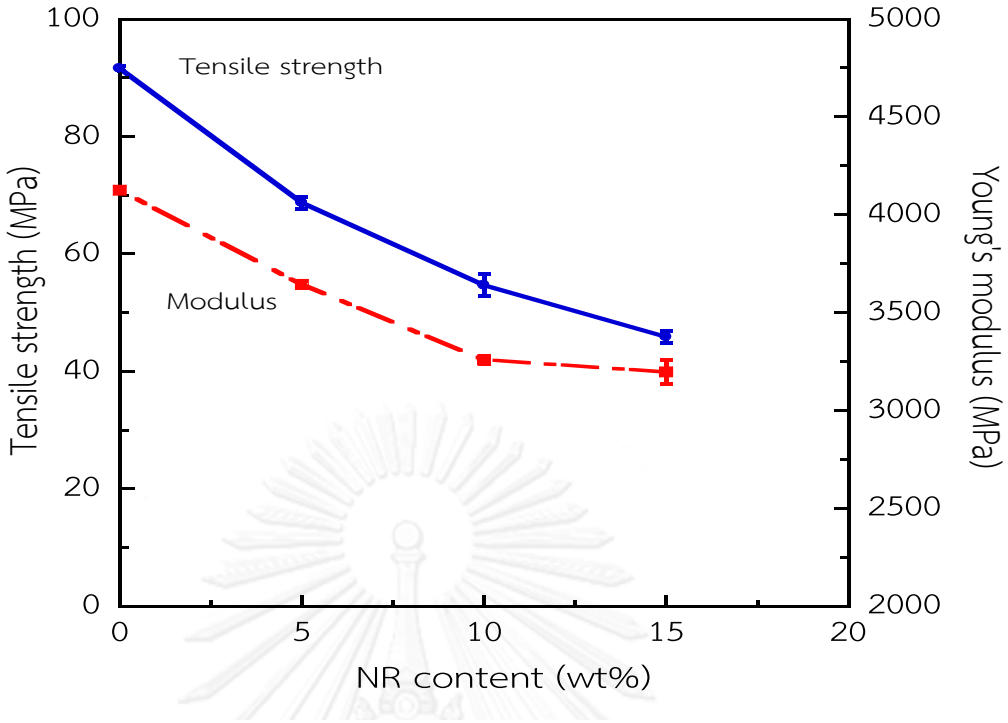

Figure 4.8 Tensile strength and Young's modulus of binary (PLA/NR) blend films

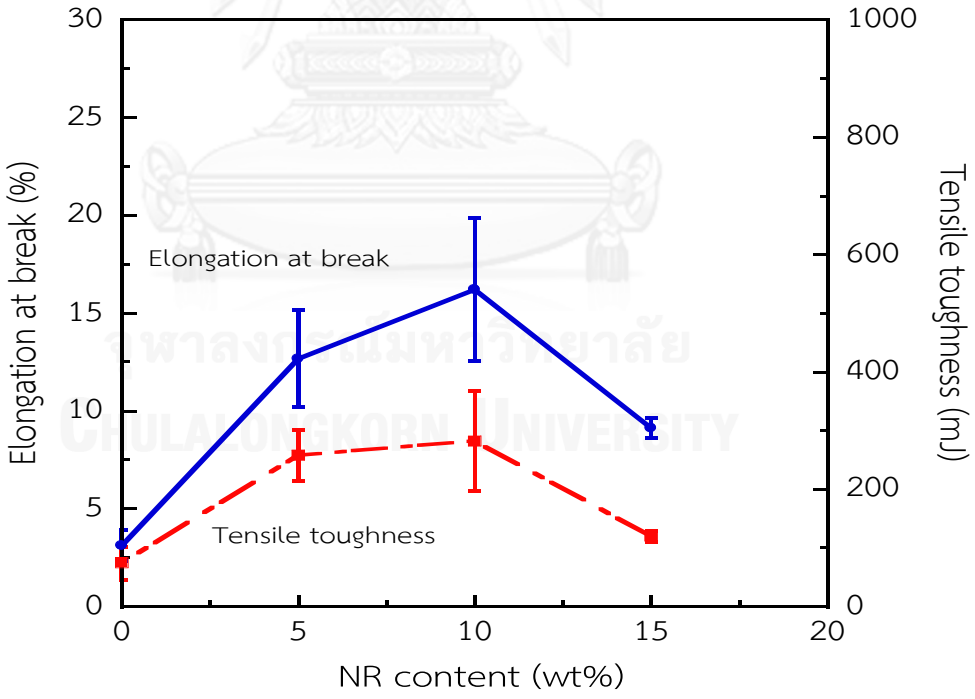

Figure 4.9 Elongation at break and tensile toughness of binary (PLA/NR) blend films

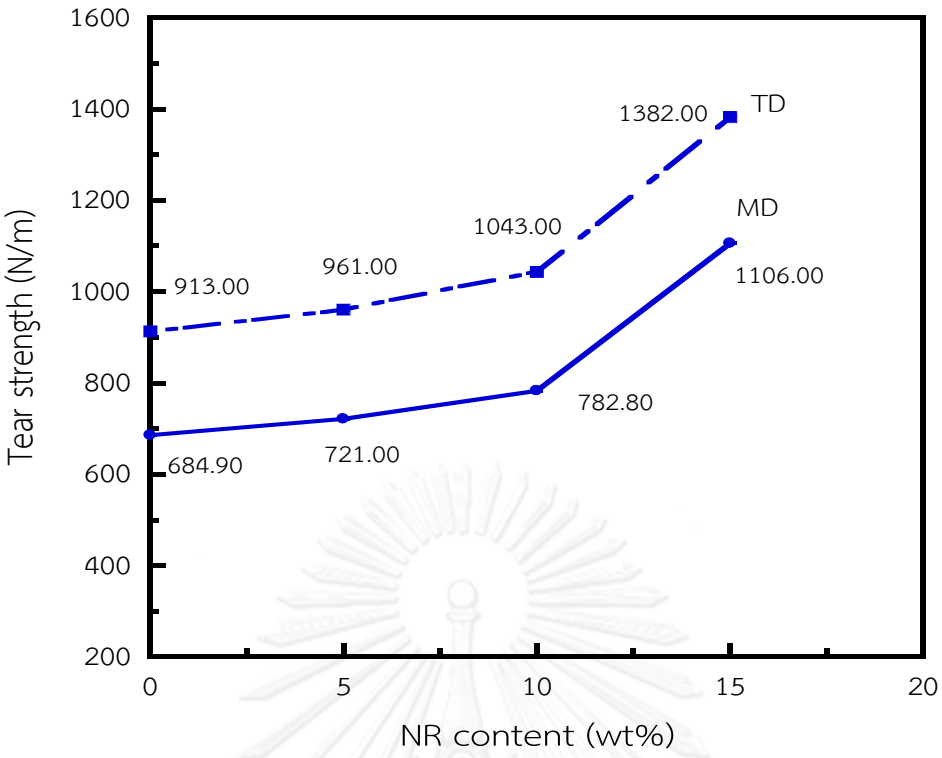

Figure 4.10 Tear strength of binary (PLA/NR) blend films

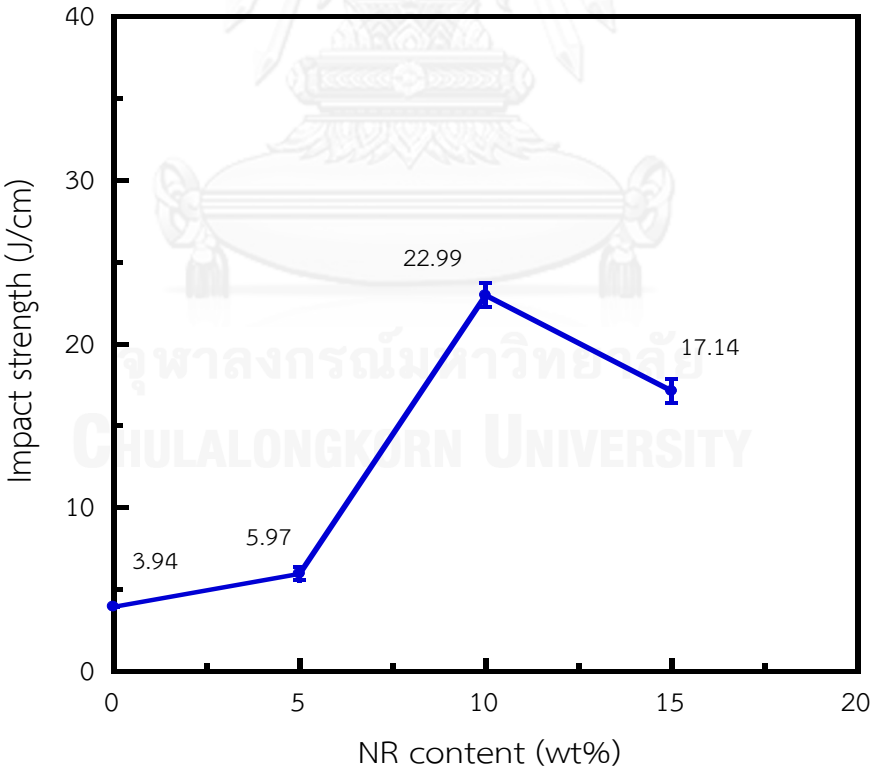

Figure 4.11 Impact strength of binary (PLA/NR) blend films

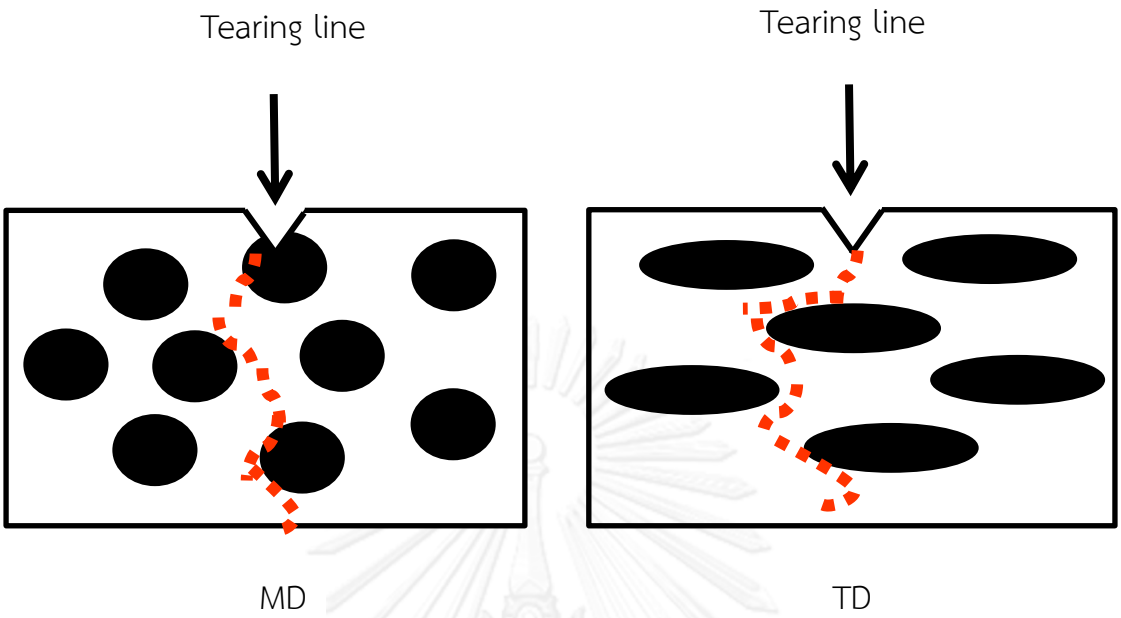

Figure 4.12 The possible tear mechanisms in PLA/NR film

4.2 Binary blend films of PLA and TPS

In this part, cassava starch and 30 wt% of glycerol were used to prepare TPS via gelatinization process in a twin screw extruder.

4.2.1 Preparation and Characterization of thermoplastic starch (TPS)

The structure of cassava starch granules and the fracture surface of TPS extrudated were observed using SEM technique as shown in Figure 4.13. The granules of cassava starch were irregular with the average size of 14.36 μm. After gelatinization process with glycerol, the granules of cassava starch were absented. It is indicated that the TPS was successfully obtained. PLA films blended with TPS at 5, 10 and 15 wt% were blown with a thickness of 40 μm. Effects of TPS content on properties of PLA blown films were implemented.

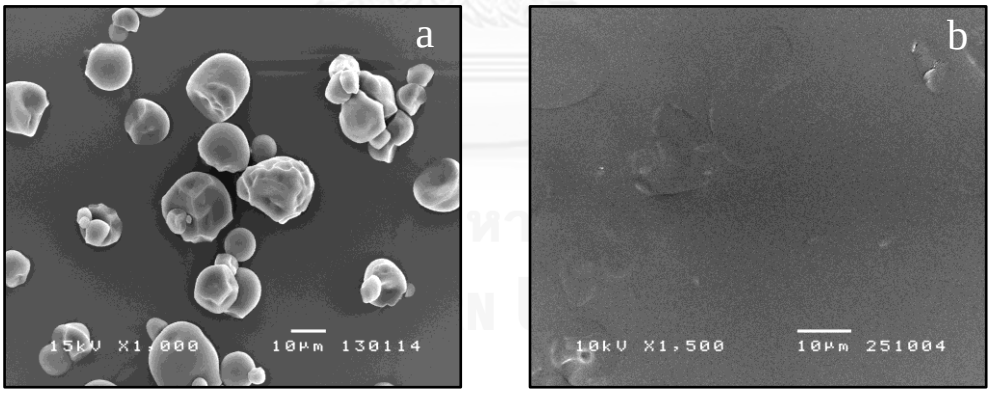

Figure 4.13 Structure of a) normal granule cassava starch and b) the TPS

4.2.2 Thermal properties

DSC curves of binary blend films are illustrated in Figure 4.14 and the analyzed data is tabulated in Table 4.3. The T_g decrease of PLA/TPS films was found as the TPS increased which the value slightly reduced from ~60 °C for neat PLA film to ~56 °C at PLA film blended with 15 wt% TPS. It is possible due to the glycerol in TPS acted as a plasticizer in PLA matrix [31]. Beside that it is believed that the decrease of T_g was a result of some degree of miscibility between PLA and TPS phases produced via a physical bonding. According to some of the previous works, the weak interaction between phases was gained through the reaction between hydroxyl groups or carboxylic acid of PLA and hydroxyl groups of TPS as demonstrated in Figure 4.15 [32, 33].

The appearance of T_{cc} peaks in PLA/TPS blend films was observed. It is mainly because a plasticizer effect of glycerol in TPS enhanced molecular chain mobility which facilitated the movement of chains from the amorphous phase to crystal phase [31, 34]. It corresponded to the shift down of T_{m1} with the presence of TPS, indicating faster crystallization.

Interestingly, the X_c of blend film increased ~2 folds for blending 5 wt% TPS compared with neat PLA film. It is pointed that the crystallization ability of PLA was enhanced due to a plasticizer effect of glycerol in TPS domains. However, the value of X_c was slightly increased with further increasing TPS content. This might be explained that a small amount of hydrolyzed products occurred during processing served as a plasticizer, increasing the chain mobility and hence the crystallinity of binary blend films. It agreed with the results reported in previous publications [35, 36].

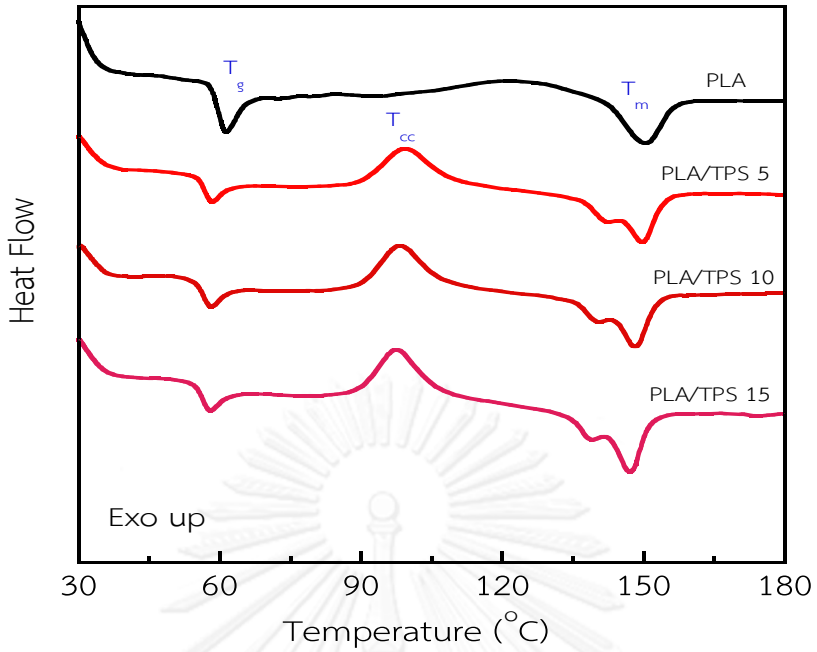

Figure 4.14 DSC thermograms in first heating scan of binary (PLA/TPS) blend films

Table 4.3 DSC data of binary (PLA/TPS) blend films

Sample	T_g	T_{cc}	T_{m2}	T_{m1}	ΔH_m	ΔH_{cc}	X_m	X_{cc}	X_c
PLA	59.5	122.6	-	150.5	14.9	12.3	16.0	13.3	2.7
PLA/TPS5	56.4	99.4	142.4	149.9	25.6	21.2	28.9	24.0	4.9
PLA/TPS10	56.1	98.4	140.6	148.3	26.8	22.4	32.1	26.8	5.2
PLA/TPS15	56.0	97.7	139.2	147.2	22.5	17.9	28.5	22.7	5.7

Note: ΔH_m - The specific melting enthalpy (J/g)

ΔH_{cc} - The specific cold crystallization enthalpy (J/g)

X_m -The degree of crystallization during melting (%)

X_{cc} - The degree of crystallization during heating (%)

X_c - The degree of crystallinity (%)

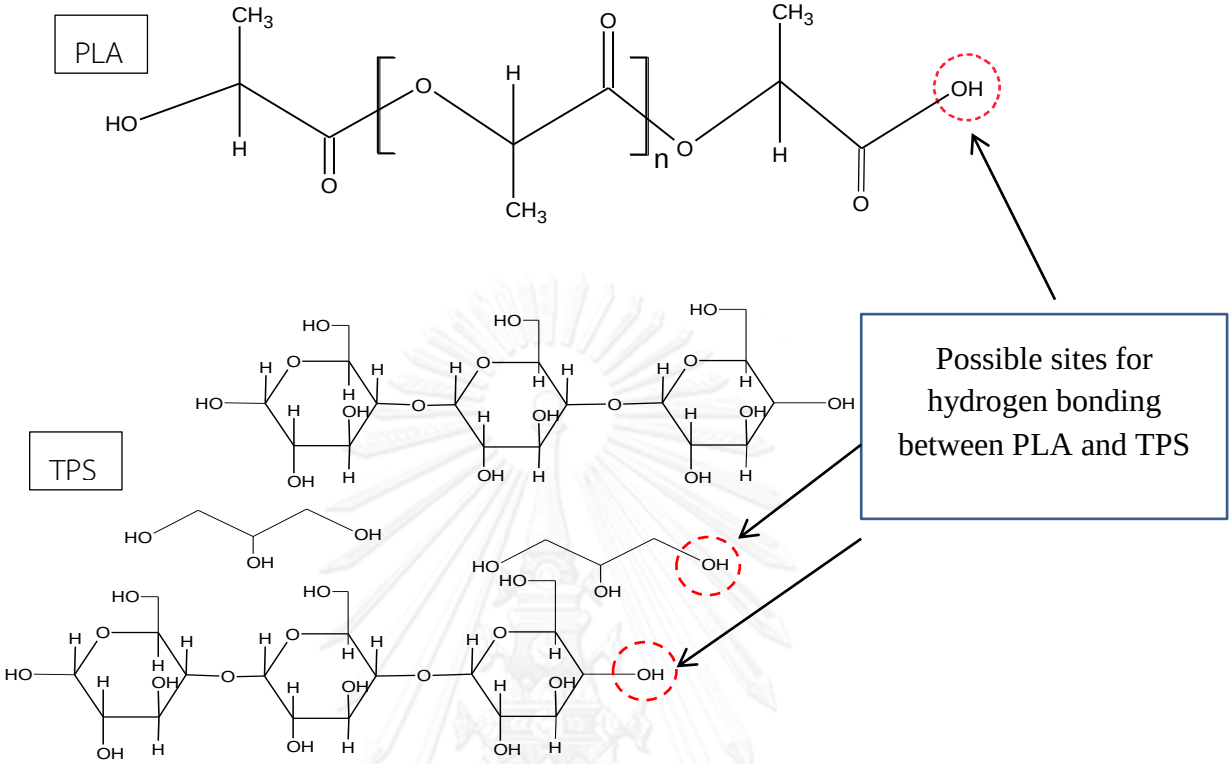

Figure 4.15 the possible site for the interaction between PLA and TPS

4.2.3 Morphology

Figure 4.16 shows the fracture surface of PLA/TPS films. Considering SEM images in MD and TD, large spherical TPS domains were visibly observed as TPS loading increased. Unfortunately, the voids, some starch granules and some gaps were also seen in SEM micrograph, especially at very high loading of TPS. The occurrence of some voids and gaps might be due to the hydrolyzed products formed during processing and the immiscible blend. As it can be seen, some TPS domains were still embedded in fracture surfaces. This is suggested that there was some interaction between PLA and TPS domains [3]. When the TPS level increased, large TPS domains were easily observed on the surface of film, resulting in a rough surface.

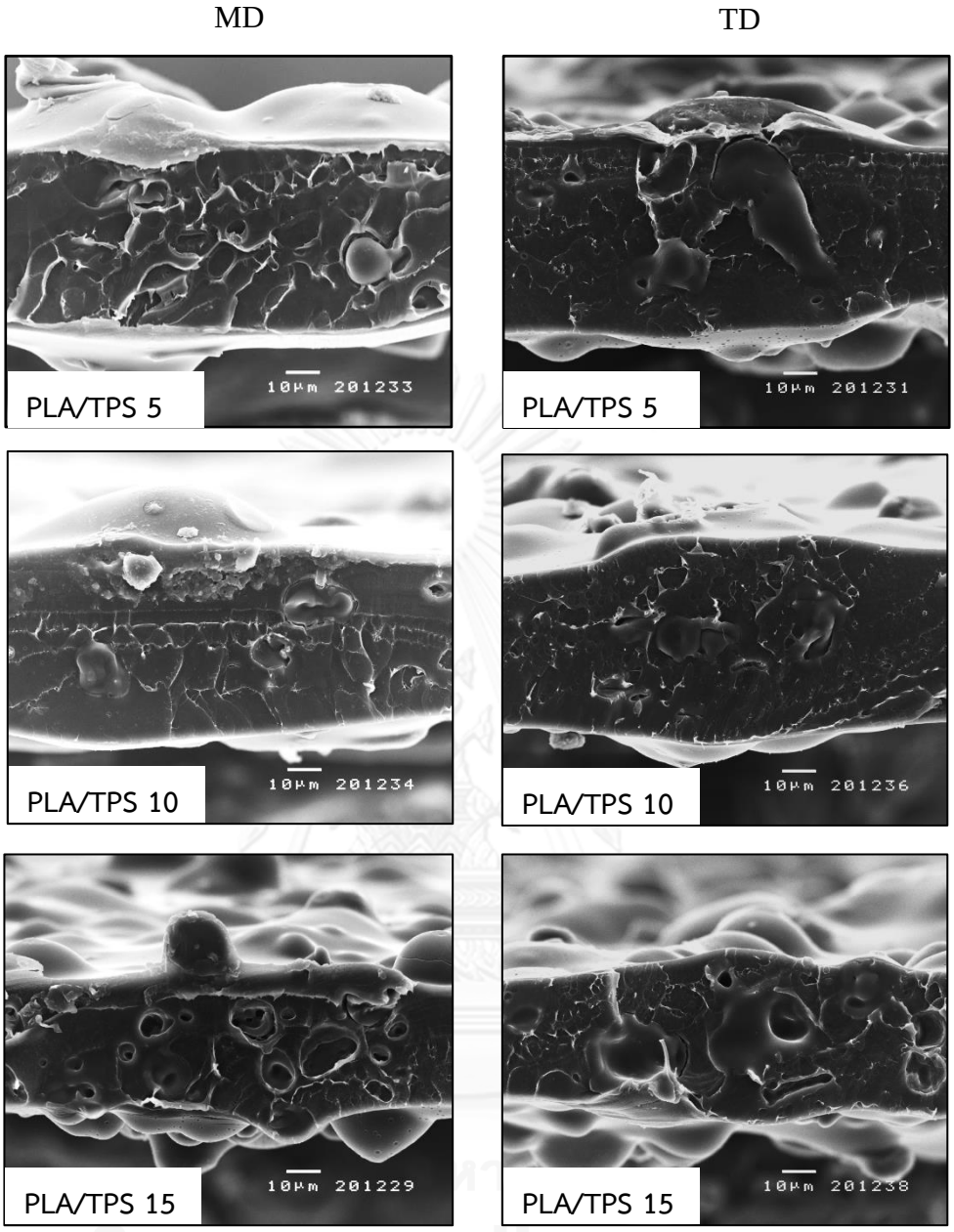

Figure 4.16 SEM micrograph of binary (PLA/TPS) blend films in MD and TD

4.2.4 Hydrophobicity and Moisture absorption

As the result of the water contact angle shown in Table 4.4, it was found that the presence of TPS fairly affected the polarity of blend films. Obviously, the water contact angle decreased from 70.76 ± 0.19 for neat PLA film to 61.36 ± 1.41 ° for PLA film blended with TPS 15 wt%. The decrement of water contact angle corresponded to the increase of hydrophilic TPS content in blend films. Furthermore, the percentage of moisture absorption increased with increasing of TPS content. Especially, the moisture absorption of PLA film blended with 15 wt% increased about 3.18 times compared with neat PLA film. It was attributed to hydroxyl group (-OH) of TPS which provided hydrogen bonding with water molecules. Moreover, the immiscible blend between PLA and TPS might generate the gaps at the interface in which the water molecules could be absorbed and stored in films [37].

Table 4.4 Water contact angle of binary (PLA/TPS) blend films

Sample	Water contact angle (°)
Neat PLA	70.76 ± 0.19
PLA/TPS5	68.97± 0.98
PLA/TPS10	62.54 ± 2.22
PLA/TPS15	61.36 ± 1.41

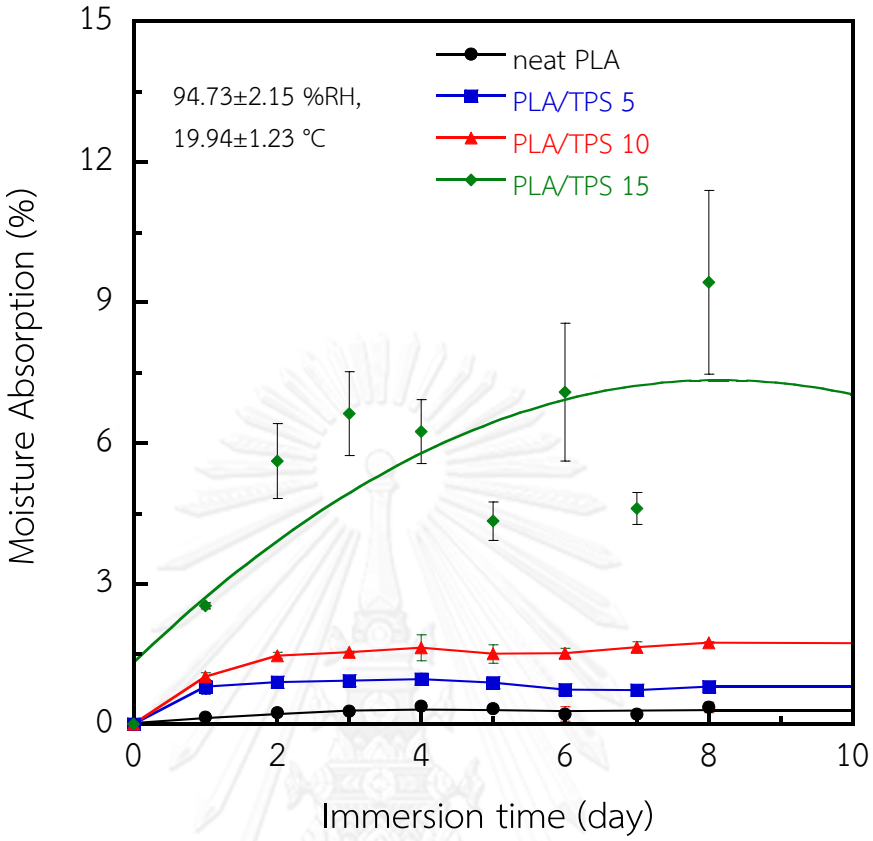

Figure 4.17 Moisture absorption of binary (PLA/TPS) blend films

4.2.5 Gas permeability properties

The values of WVP and OP of PLA blended with various TPS contents are depicted in Figure 4.18. Owing to enhanced hydrophilic characteristic of PLA/TPS films as mentioned above, WVP values linearly increased as a function of TPS content. The molecules of water vapor more preferred to saturate at the hydrophilic surface and then move through the films, resulting in high water vapor transmission rate. For the permeability of O_2, the OP value slightly increased for PLA film blended with TPS 5 wt%. It might be due to the increase of free volume caused by the phase-separated structure of PLA/TPS blend. However, the permeability strongly dropped at higher TPS loading. It is mainly because the surface of blend films was covered with a thin layer of water vapor molecules generated in a humidity chamber (90 %RH), hindering the permeability of the nonpolar oxygen molecules through the films [38].

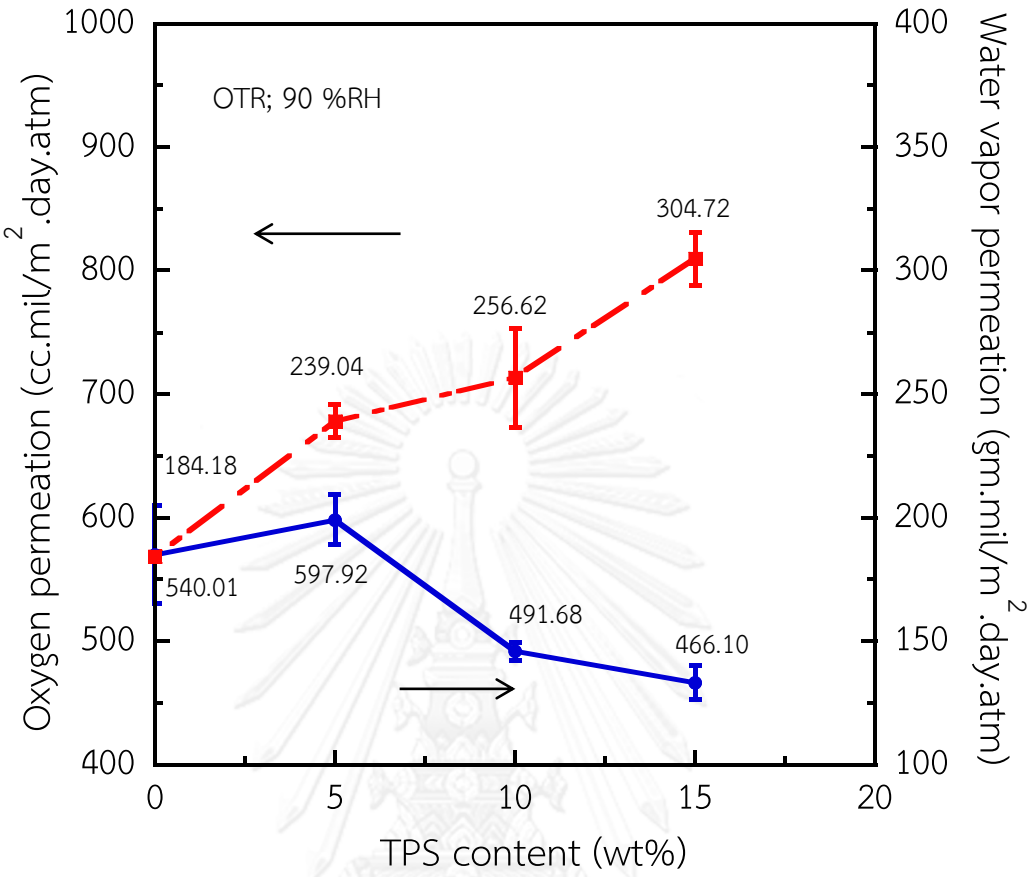

Figure 4.18 Oxygen and water vapor permeation of binary (PLA/TPS) blend films

4.2.6 Mechanical properties

The effect of TPS content on mechanical properties of blend films is presented in Figure 4.19. Young's modulus and tensile strength of PLA/TPS blend films in MD decreased about 21.45% and 41.50%, respectively, as shown in Figure 4.21. This indicates that PLA/TPS films were less stiff and easy to deform because of the effect of soft TPS and immiscible blend [6].

Figure 4.22 displays elongation at break and tensile toughness also decreased when the amounts of TPS increased thus the plastic deformation zone was very small visible in the stress-strain curve of PLA/TPS films. It is probably due to the crack initiation often generated from the large TPS domains in films [39]. The fracture surface of stretched PLA/TPS films after tensile testing is demonstrated in Figure 4.20. The deformed specimens show the brittle failure like neat PLA film, primarily because TPS could not absorb and dissipate the applied energy.

Additionally, tear strength and impact strength of blend films decreased with increasing of TPS loading as respectively displayed in Figure 4.23 and Figure 4.24. It was attributed to the immiscible blend of PLA and TPS with low interfacial interaction. Accordingly, large TPS domains would be a stress concentrator in which the crack propagation was formed. It might be related to the fact that large TPS domains could not absorb and dissipate the applied energy as well [40].

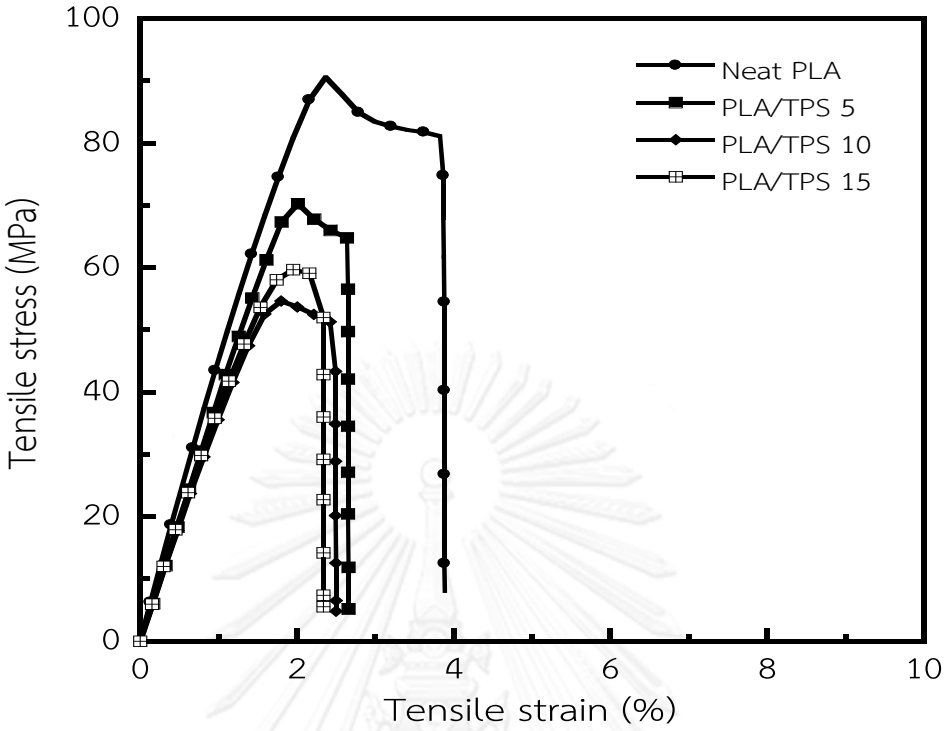

Figure 4.19 Stress-strain curve of of binary (PLA/TPS) blend films

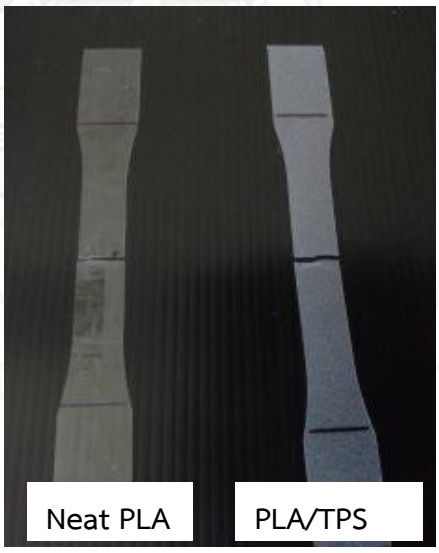

Figure 4.20 The photograph of deformed specimens after tensile testing of neat PLA and PLA/TPS10 film

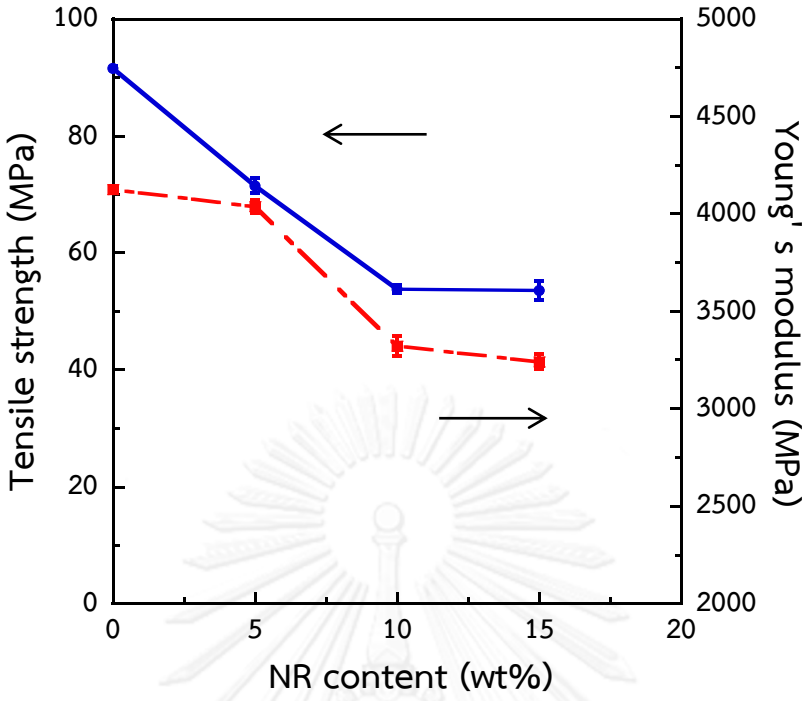

Figure 4.21 Tensile strength and Young's modulus of binary (PLA/TPS) blend films

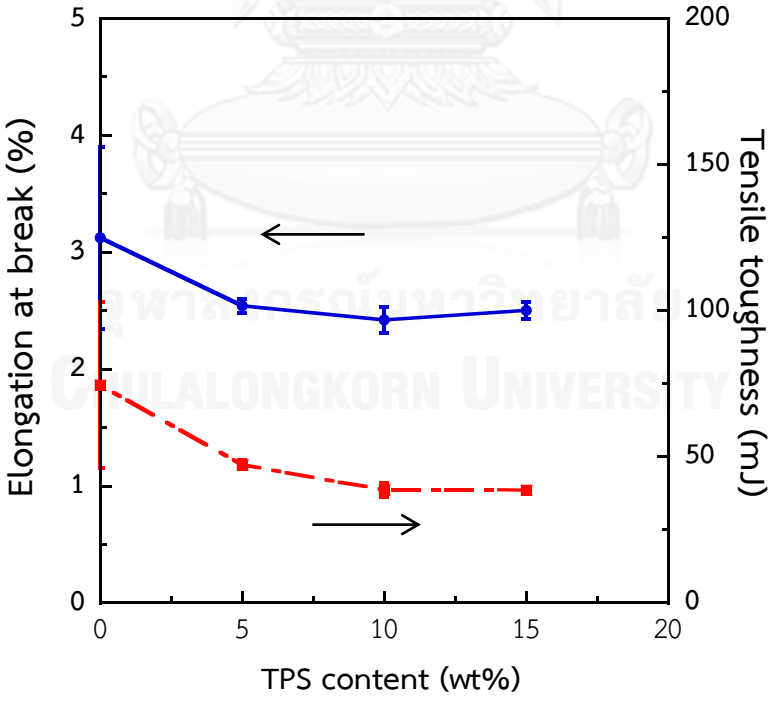

Figure 4.22 Elongation at break and Tensile toughness of binary (PLA/TPS) blend films

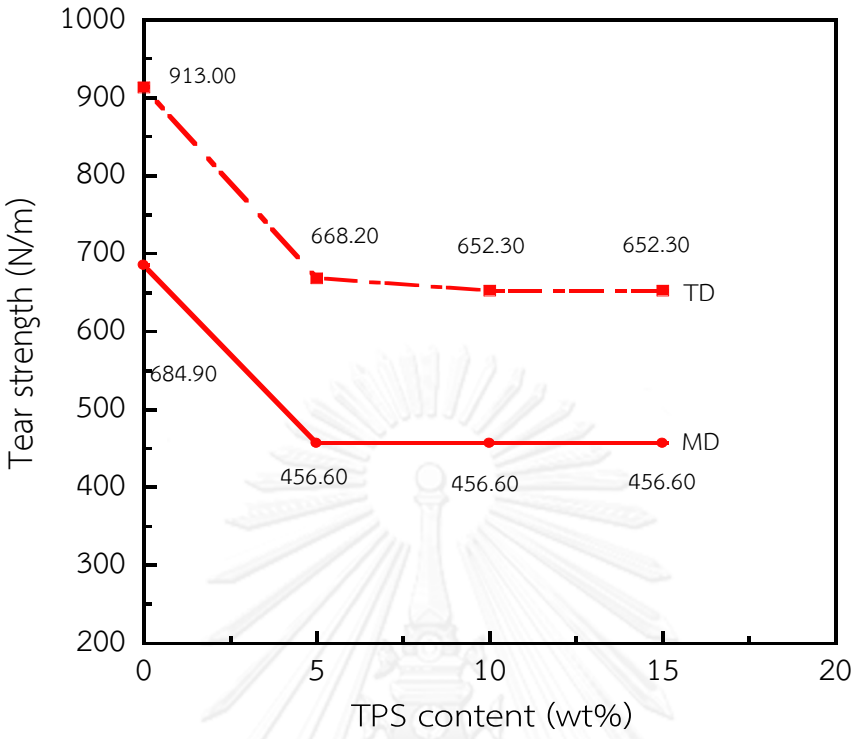

Figure 4.23 Tear strength of binary (PLA/NR) blend films

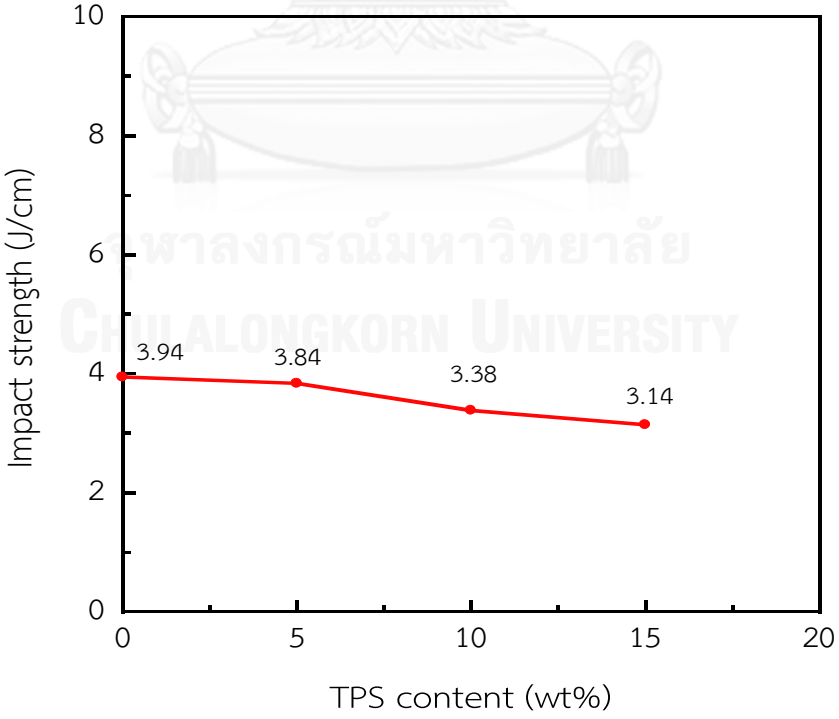

Figure 4.24 Impact strength of binary (PLA/TPS) blend films

4.3 Ternary blend films of PLA, NR and TPS

As the result as aforementioned, binary blend film of PLA/NR10 provided the enhancement of toughness and mechanical properties that are one of the most important properties for packaging application. Therefore, PLA/NR10 film is a reference film in this section. For TPS, it exhibited high performance for achieving the moisture absorption and WVP of PLA films blended with TPS. Consequently, TPS was chosen to use in this section in order to improve the moisture sensitivity of blown films. Ternary blend films were produced which the NR content was fixed at 10 wt% and the TPS content was varied at 5, 10, 15 wt%. The various properties of ternary blend films were investigated and compared with a reference film.

4.3.1 Thermal properties

DSC thermograms of ternary blend films in the first heating are depicted in Figure 4.25 and the analyzed results are summarized Table 4.6. The T_g of ternary blend films was slightly decreased with increasing TPS content. The T_g value reduced from ~59°C for a reference film, which is PLA/NR10 film, to ~56°C for blend film of PLA/NR10/TPS15. This is due to the plasticizer effect of glycerol in TPS and the hydrolyzed products as aforementioned [35, 36].

The exothermic peak of T_{cc} for all ternary blend films was narrower and shifted to lower temperature when TPS content increased. It can be described by the fact that the glycerol and the hydrolyzed products acted as the nucleating agent, inducing faster crystallization and enhancing the crystallization ability in PLA/NR matrix. Moreover, the T_{cc} of ternary blend films were shifted to lower temperature than the T_{cc} of binary (PLA/TPS) blend films. This is because the glycerol content in

TPS of ternary blend has higher when compared with binary blend. The comparison of TPS content was reported in Table 4.5. Double melting peaks were still observed in ternary blend films. Interestingly, the T_{m1} of these blend films was very small like a shoulder of main melting peak compared with a reference film. It is due to the less crystals forming during the cold crystallization with increasing TPS concentration, which corresponded to the decrease of ΔH_{cc}. The X_c of ternary blend films was insignificantly changed as TPS content increased. It is probably due to the fact that the decrease of PLA concentration reduced the crystallization ability in PLA matrix. Another assumption is that NR domains might inhibit the potential of the plasticizer and the nucleating agents derived from PLA and TPS.

Table 4.5 Comparison of glycerol content in binary and ternary blend films

Sample	Content (wt%)			GLY:PLA (%)
	PLA	TPS	Glycerol	
PLA/TPS5	95	5	1.5	1.58
PLA/TPS10	90	10	3.0	3.33
PLA/TPS15	85	15	4.5	5.30
PLA/NR10/TPS5	85	5	1.5	1.76
PLA/NR10/TPS10	80	10	3.0	3.75
PLA/NR10/TPS15	75	15	4.5	6.00

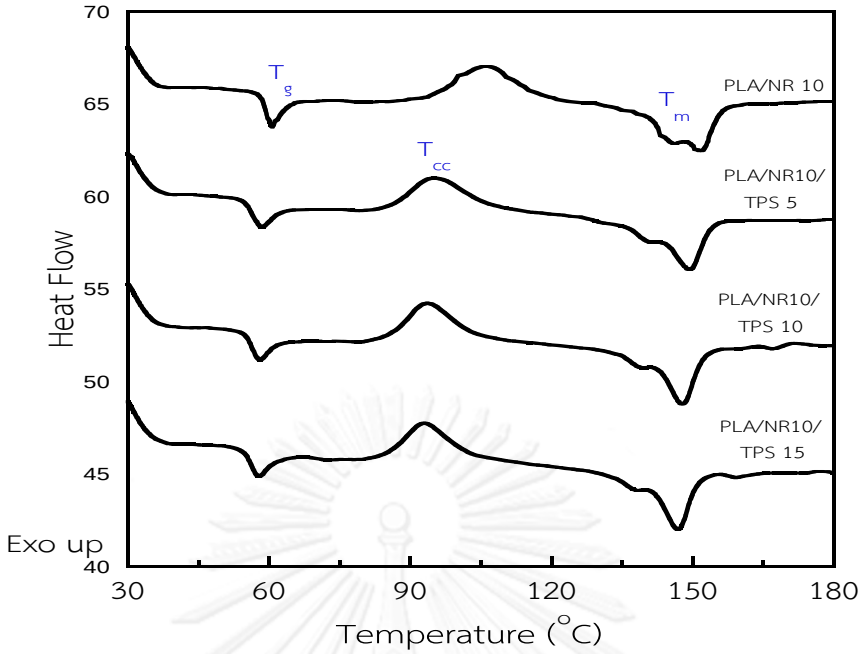

Figure 4.25 DSC thermogram of ternary (PLA/NR10/TPS) blend films

Table 4.6 DSC data of ternary (PLA/NR10/TPS) blend films

Sample	T_g	T_{cc}	T_{m1}	T_{m2}	ΔH_m	ΔH_{cc}	X_m	X_{cc}	X_c
PLA/NR10	59.2	106.6	146.3	151.8	21.9	17.9	16.0	13.3	2.7
PLA/NR10/TPS5	56.2	94.9	141.0	149.1	22.8	19.2	26.1	21.4	4.7
PLA/NR10/TPS10	56.2	93.6	138.7	147.8	21.2	17.7	28.9	24.2	4.6
PLA/NR10/TPS15	55.9	92.8	137.8	146.8	20.3	16.9	28.6	23.8	4.8

Note: ΔH_m - The specific melting enthalpy (J/g)

ΔH_{cc} - The specific cold crystallization enthalpy (J/g)

X_m -The degree of crystallization during melting (%)

X_{cc} - The degree of crystallization during heating (%)

X_c - The degree of crystallinity (%)

4.3.2 Morphology

As expected, SEM micrographs of ternary blend films in Figure 4.26 show the characteristic of phase separation which the components of PLA, NR and TPS were clearly evident. It can be seen that the fracture surface was very rough probably due to multi-components and multi-interaction between phases. Observiously, TPS domains were bigger than NR domains, and they were mostly embedded in both surfaces of ternary blend film. Therefore, the roughness of blend films strongly increased as TPS loading increased. Figure 4.27 illustrates the high resolution of SEM image for ternary blend film. It can be seen that some TPS domains were covered with NR domains, resulting in loss of their surface area.

MD TD

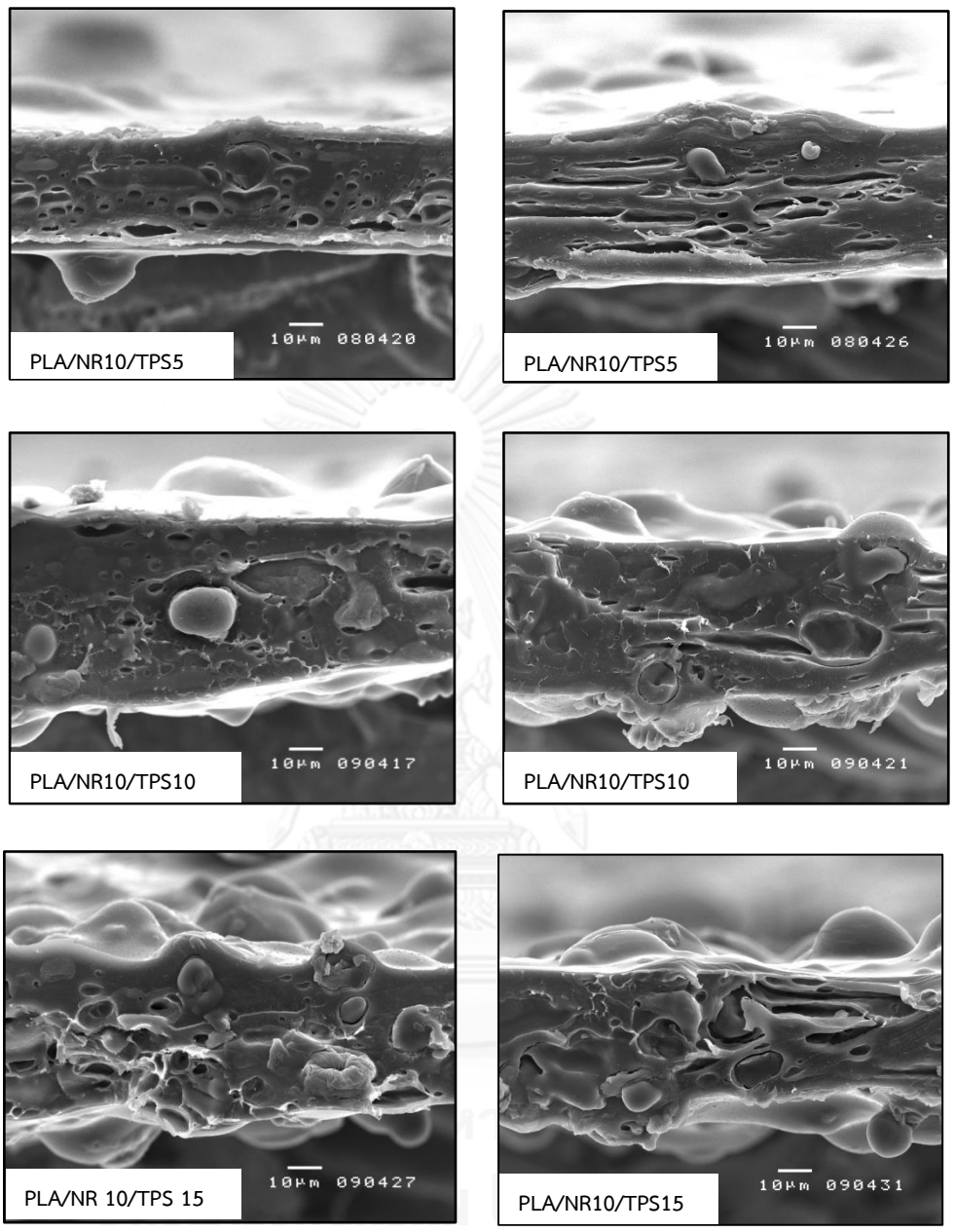

Figure 4.26 SEM micrographs of fracture surface of ternary (PLA/NR10/TPS) blend films in MD and TD

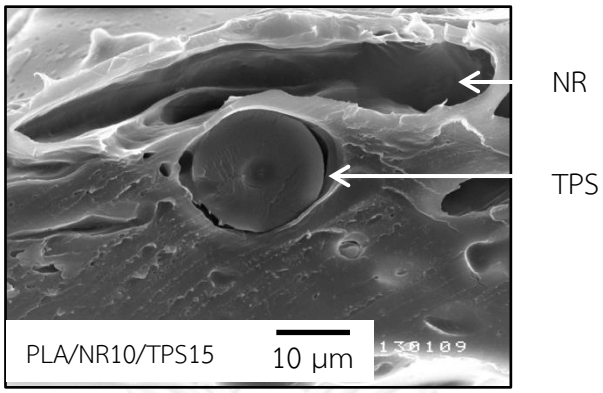

Figure 4.27 SEM micrograph of PLA/NR10/TPS15 domain in PLA matrix

4.3.3 Hydrophobicity and Moisture absorption

The moisture absorption curve as demonstrated in Figure 4.28, a rapid water uptake for the initiate period of immersion time was noticeably observed for ternary blend films, especially at high TPS loading. The water molecules were immersed and stored in the interphases between PLA, NR and TPS of ternary blend films. Moreover, water molecules were constructively absorbed in hydrophilic TPS portion via hydrogen bonding between hydroxyl group of TPS and water molecule [37]. However, the percentage of moisture absorption of ternary blend films was lower than that of binary blend films of PLA/TPS. It is mainly because some part of TPS domains was adhered by NR domains as mentioned previously, reducing the absorption of water vapor molecules. Besides, the water contact angle of ternary blend films decreased with increasing of TPS content because of the hydrophilic characteristic of TPS.

Table 4.7 Water contact angle of ternary (PLA/NR10/TPS) blend films

Sample	Water contact angle (°)
PLA/NR 10	73.95 ± 0.01
PLA/NR10/TPS 5	71.11 ± 0.95
PLA/NR10/TPS 10	70.62 ± 2.53
PLA/NR10/TPS 15	68.67 ± 2.12

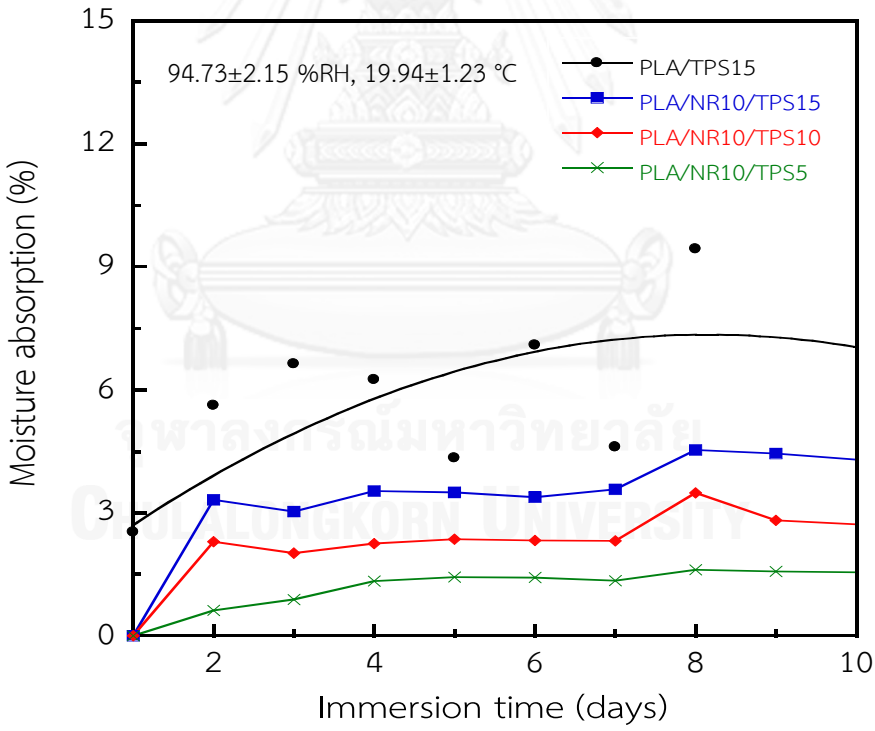

Figure 4.28 Moisture absorption curves for ternary (PLA/NR10/TPS) blend films and PLA/TPS15 blend films

4.3.4 Gas permeability properties

It is known that gas molecules could diffuse through the voids or a free volume of films which were usually created by the immiscible blends. However, the chemical affinity which can be defined by the interaction of that gas in films is an important factor for gas transmission [17]. Ternary blend films having more polarity would resist the diffusion of non-polar molecules such as oxygen. Thus, the OP values of blend films mixed with TPS were lower than those of PLA/NR blend films as shown in Figure 4.29. Additionally, the WVP value gradually increased as TPS loading increased. The WVP value of PLA/NR10/TPS15 film increased about 25% and 36% when was compared with PLA/NR10 and neat PLA films, respectively. This is again due to the effect of hydrophilic characteristic and chemical affinity between water molecules and TPS domains.

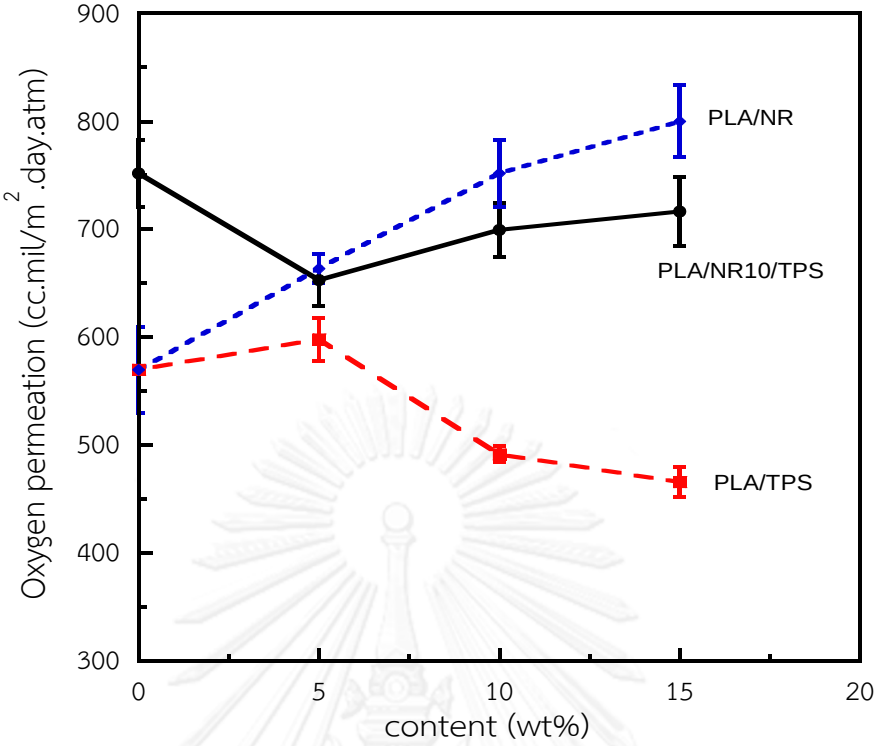

Figure 4.29 Oxygen permeation of ternary (PLA/NR10/TPS) blend films

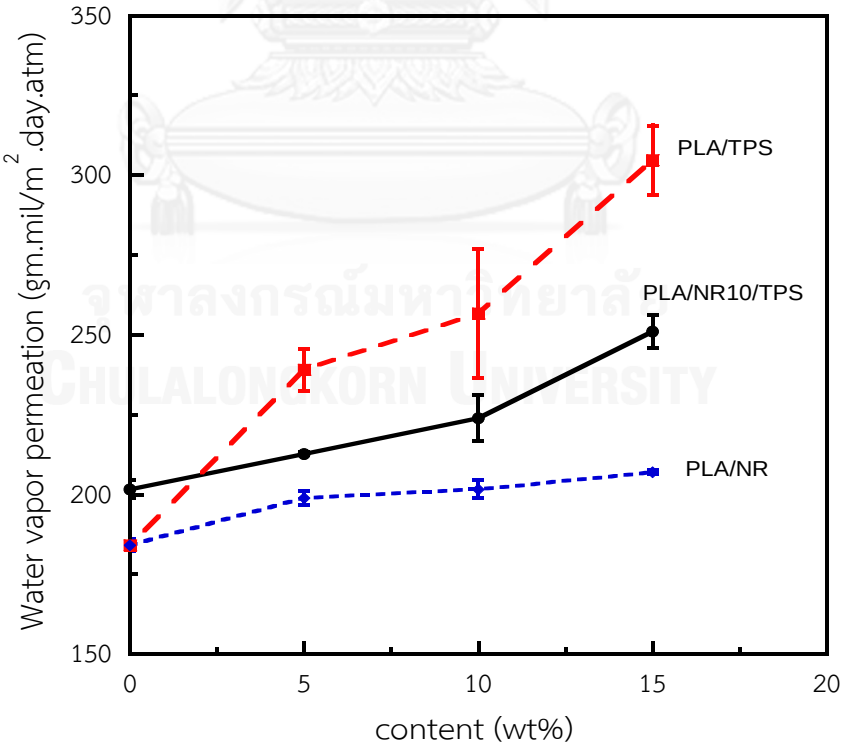

Figure 4.30 Water vapor permeation of ternary (PLA/NR10/TPS) blend films

4.3.5 Mechanical properties

Tensile properties of PLA/NR/TPS films were found to decrease as shown in Figure 4.32. Tensile strength decreases 33.33 % for the corporation of 15 wt% of TPS because low interfacial interaction and inefficiency of TPS on ability of absorption and dispersion stress [37]. Young's modulus is also decrease to 24.49 % for PLA/NR10/TPS15 film as demonstrate in Figure 4.33. This is associated to the effect of adding NR domain and soft TPS which has glycerol contents. The effect of NR and TPS in PLA matrix on elongation at break and tensile toughness of PLA/NR/TPS films were shown in Figure 4.34. It was found to decrease because the large TPS domain inhibits to transfer the stress and poor interfacial adhesion between PLA, NR and TPS phases. However, the elongation at break of ternary blends was still higher than that of PLA/TPS blend films because of the elastic properties of NR domain. This result was discussed in detail as illustrated in Figure 4.32.

Tear strength of ternary films increased when adding of 5 wt% TPS. This is because at low content of TPS, TPS can well disperse in PLA/NR matrix which leads to more crack length. Therefore, the higher energy of tearing required to tears the ternary films. However, the tear strength decreased with higher of TPS content. This may be suggested that TPS domain contacted together or NR domain which induced large zone at the crack tip blunted the crack and prevented.

Considering of impact strength, the values of impact strength were also decreased with the corporation of TPS contents as shown in Figure 4.36. The decrement of the impact strength is related to the large size of TPS which is not absorbed and dissipated the applied energy.

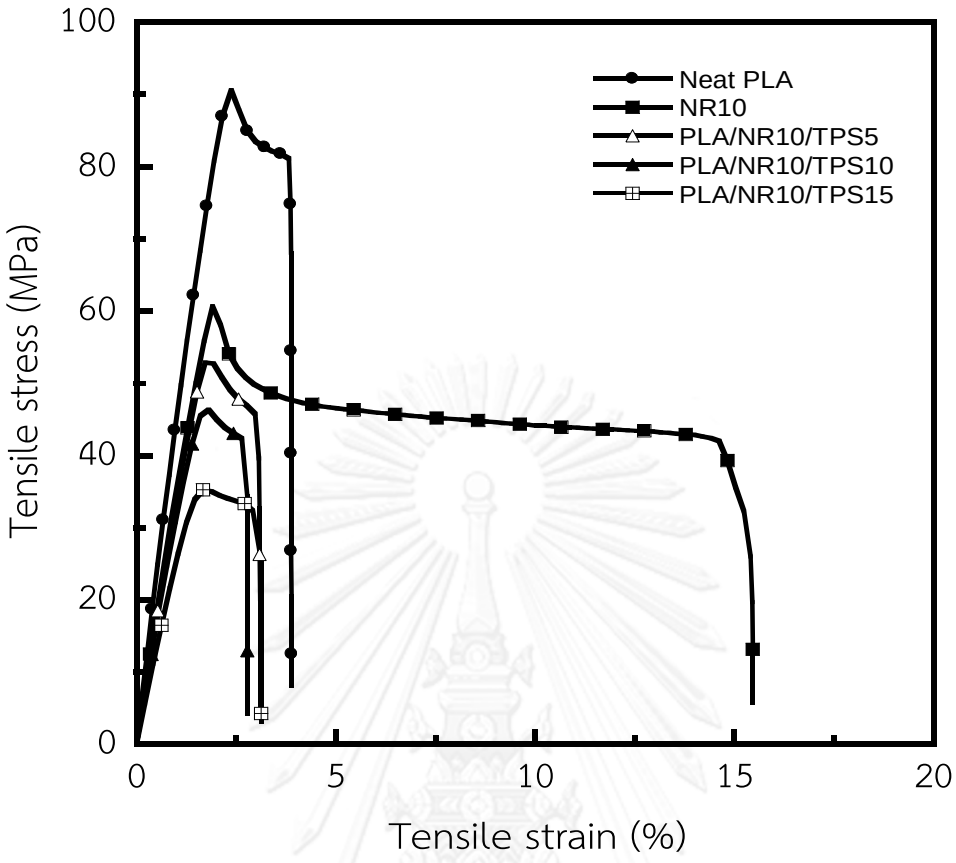

Figure 4.31 Stress-strain curve of ternary (PLA/NR10/TPS) blend films

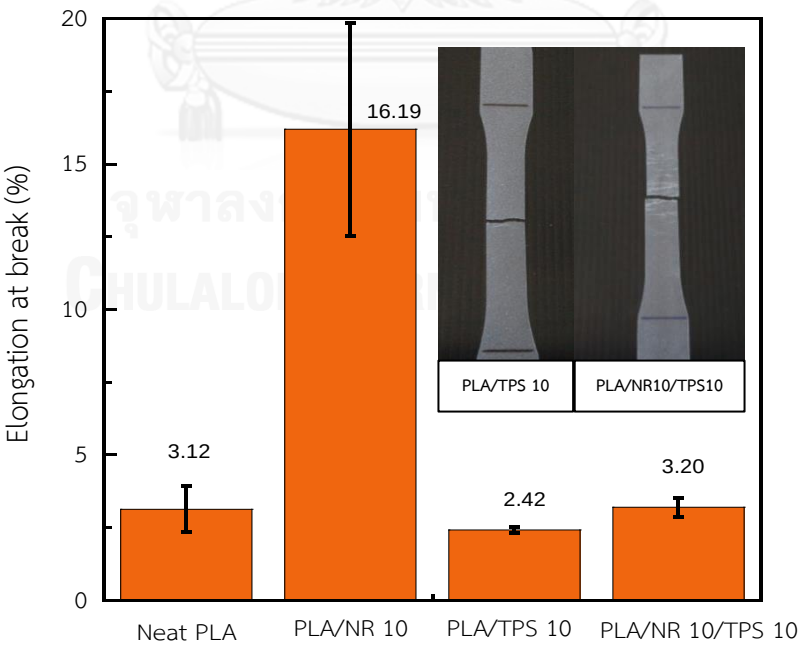

Figure 4.32 Comparison of Elongation at break of binary and ternary blends

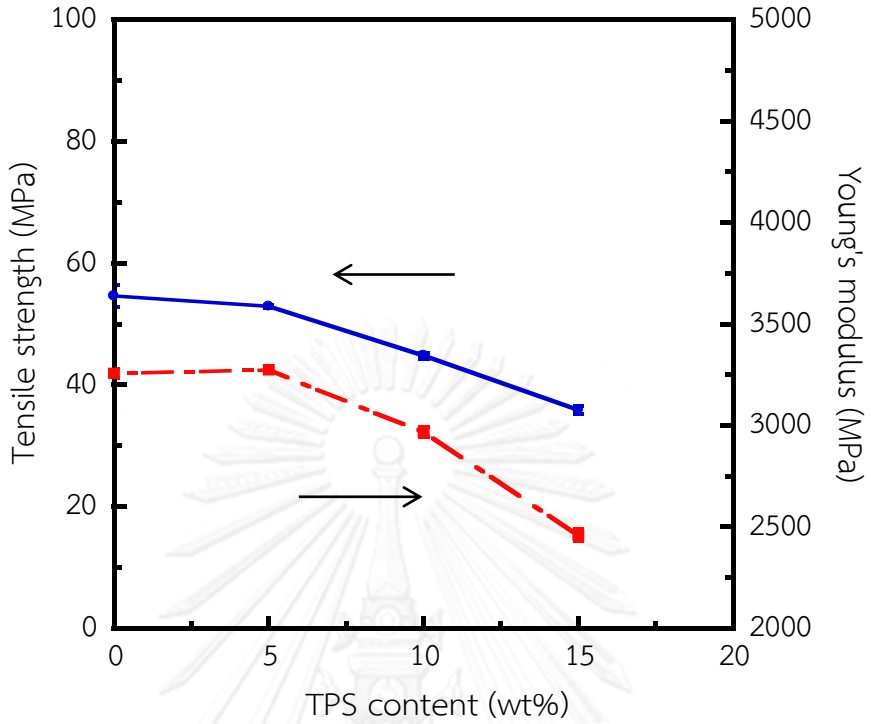

Figure 4.33 Tensile strength and Young's modulus of ternary (PLA/NR/TPS) blend films

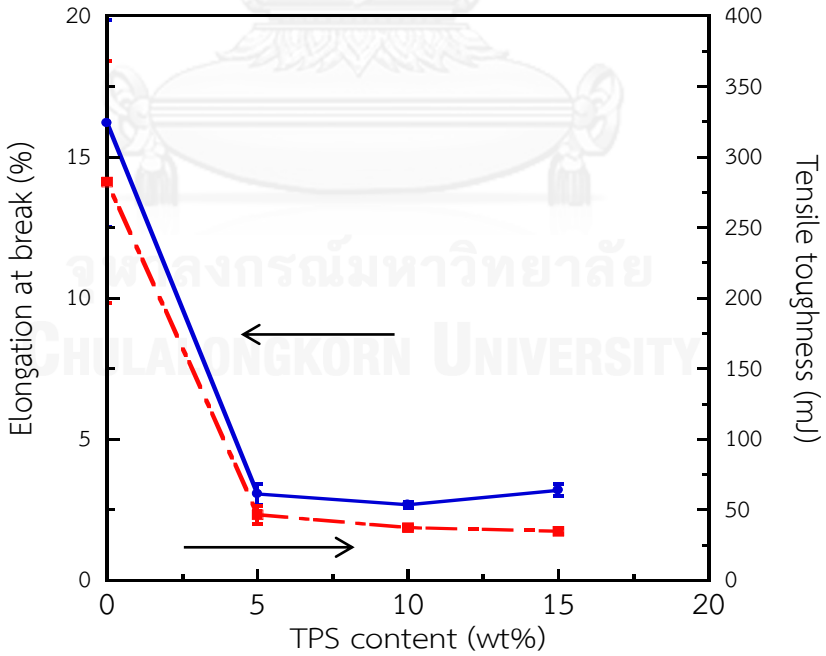

Figure 4.34 Elongation at break and Tensile toughness of ternary (PLA/NR/TPS) blend films

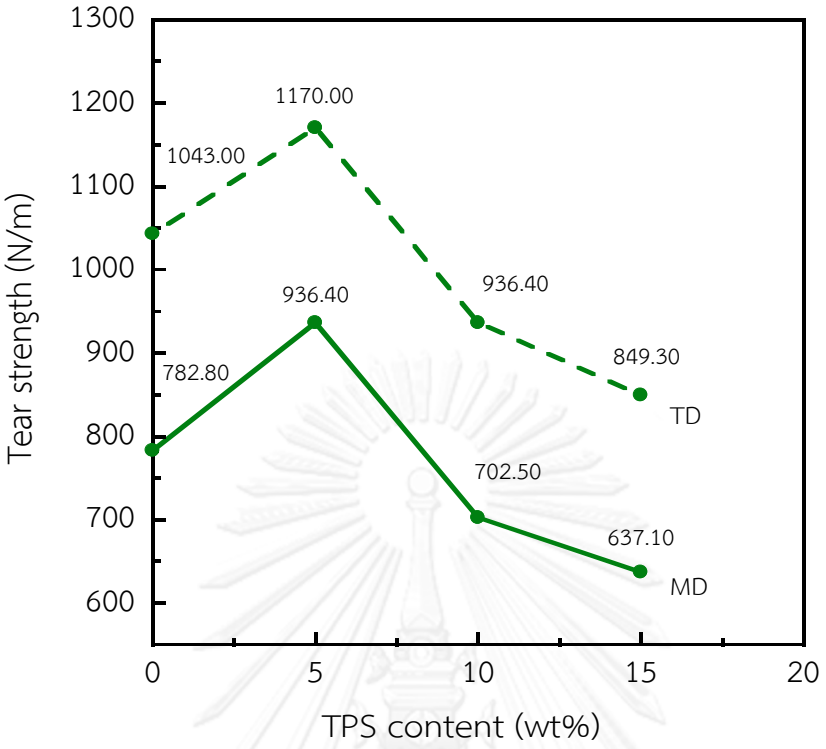

Figure 4.35 Tear strength of ternary (PLA/NR/TPS) blend films

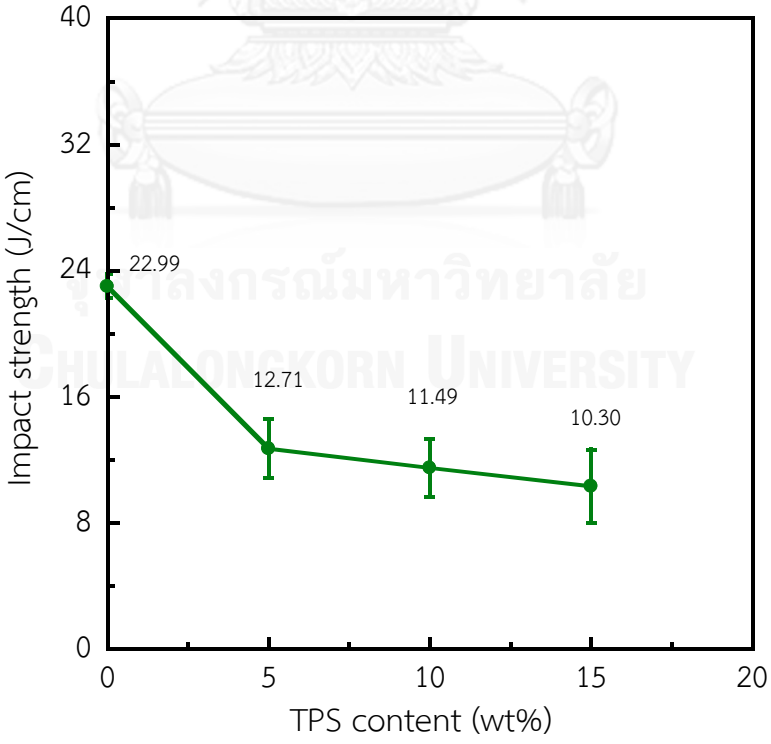

Figure 4.36 Impact strength of ternary (PLA/NR/TPS) blend films

CHAPTER V

CONCLUSIONS AND RECOMMENDATION

5.1 Conclusions

From the primary purpose of this research, the property development of PLA blown films for using in green packaging application, especially for fresh produces, was focused. Therefore, the effect of the presence of natural rubber (NR) and thermoplastic starch (TPS) in binary and ternary blends in PLA-based blown films was considered on thermal, physical and mechanical properties. The following major conclusions can be drawn from these results.

For binary blends, PLA/NR and PLA/TPS blown films were productively equipped. Dispersed NR domains acting as a nucleating agent could effectively induce faster crystallization and high crystallinity percentage (X_c) in PLA/NR blend films. Oxygen permeability enhancement in PLA/NR blown films was obviously achieved as well. The toughness and mechanical properties of PLA blown film were intensely improved by blending with only 10 wt% NR.

Moreover, TPS was successfully prepared from 70 wt% cassava starch and 30 wt% glycerol via the gelatinization process in the twin screw extruder. The presence of low-molecular-weight glycerol in TPS greatly enhanced the crystallization ability in blown films. Comparing with neat PLA film, the value of X_c increased approximately two times for binary blend film of PLA/TPS5. Moisture absorption and water vapor

permeation of PLA/TPS blend films were remarkably developed, especially at 15 wt% TPS.

For ternary blend films, NR content was fixed at 10 wt% and TPS loading was varied. Hydrophilic characteristic of PLA/NR10/TPS films was noticeably improved, corresponding to the decrease in water contact angle with increasing TPS content. Besides, the existence of TPS in ternary blend films substantially affected high rate of moisture absorption. Moisture absorption of PLA/NR10/TPS15 film was extremely higher than that neat PLA film about 13 folds.

Accordingly, ternary blend films generated by blending PLA with NR and TPS are very interesting candidate for green packaging application for fresh produces. Due to the outstanding performance of blend films which rate of moisture absorption was extremely high, the problem about the cumulative moisture from the respiration of fresh produces in packaging might be overcome.

5.2 Recommendation

- Considering gas permeation, the quantity of voids and the thickness of films are the main effects. The increase of voids in thin film may be conducted by removing the dispersed domains that adsorbed on the surface of films via the suitable processes such as hot water dissolution
- Because each fresh produces has different rate of respiration, the proper films should be tested in real condition for extended shelf life of each one.
- In moisture absorption part, the weighting process should be conducted in a closed system for the accurate data.

REFERENCES

[1] Zhang, C., Man, C., Pan, Y., Wang, W., Jiang, L., and Dan, Y., Toughening of polylactide with natural rubber grafted with poly(butyl acrylate). Polymer International, 2011. 60(10): p. 1548-1555.

[2] Bitinis, N., Verdejo, R., Cassagnau, P., and Lopez-Manchado, M.A., Structure and properties of polylactide/natural rubber blends. Materials Chemistry and Physics, 2011. 129(3): p. 823-831.

[3] Yew, G.H., Mohd Yusof, A.M., Mohd Ishak, Z.A., and Ishiaku, U.S., Water absorption and enzymatic degradation of poly(lactic acid)/rice starch composites. Polymer Degradation and Stability, 2005. 90(3): p. 488-500.

[4] *Describe why food spoils*. [cited 2014 25 April]; Available from: http://www.foodsafetysite.com/educators/competencies/general/spoilage/spg1.html.

[5] Hablot, E., Dewasthale, S., Zhao, Y., Zhiguan, Y., Shi, X., Graiver, D., and Narayan, R., Reactive extrusion of glycerylated starch and starch-polyester graft copolymers. European Polymer Journal, 2013. 49(4): p. 873-881.

[6] Raj, B., Sankar, U.K., and Siddaramaiah, Low density polyethylene/starch blend films for food packaging applications. Advances in Polymer Technology, 2004. 23(1): p. 32-45.

[7] Olivato, J.B., Grossmann, M.V.E., Yamashita, F., Nobrega, M.M., Scapin, M.R.S., Eiras, D., and Pessan, L.A., Compatibilisation of starch/poly(butylene adipate co-terephthalate) blends in blown films. International Journal of Food Science and Technology, 2011. 46(9): p. 1934-1939.

[8] Jagannath, J.H., Nadanasabapathi, S., and Bawa, A.S., Effect of starch on thermal, mechanical, and barrier properties of low density polyethylene film. Journal of Applied Polymer Science, 2006. 99(6): p. 3355-3364.

[9] *European bioplastics*. [cited 2013 29 December]; Available from: http://en.european-bioplastics.org/market/.

[10] Suksut, B. and Deeprasertkul, C., Effect of Nucleating Agents on Physical Properties of Poly(lactic acid) and Its Blend with Natural Rubber. Journal of Polymers and the Environment, 2011. 19(1): p. 288-296.

[11] Ketwattha, U. and Somwangthanaroj, A. The development of toughness and gas permeability of Poly(lactic acid)/maleic anhydride-g-natural rubber blown film. Chulalongkorn University, 2011.

[12] Perkins W. G., Polymer Toughness and Impact Resistance. Polymer Engineering and Science, 1999. 39(12): p. 2445-2459.

[13] Sperling L.H., Introduction to physical polymer science, ed. 4th. 2006.

[14] Averous, L., Biodegradable Multiplephase System Based on Plasticized Starch: A Review. Journal of Macromolecular Science, 2004. C44: p. 231-274.

[15] Srirod, K. and Piyajomkwan, K., Technology of starch, ed. 3. 2003: Kasetsart University Press.

[16] Kahar, A.W.M., Ismail, H., and Othman, N., Properties of HVA-2 vulcanized high density polyethylene/natural rubber/thermoplastic tapioca starch blends. Journal of Applied Polymer Science, 2013. 128(4): p. 2479-2488.

[17] Bastani, D., Esmaeili, N., and Asadollahi, M., Polymeric mixed matrix membranes containing zeolites as a filler for gas separation applications: A

review. Journal of Industrial and Engineering Chemistry, 2013. 19(2): p. 375-393.

[18] Mittal, V., Crystallinity, mechanical property and oxygen permeability of polypropylene: Effect of processing conditions, nucleating agent and compatibilizer. Journal of Thermoplastic Composite Materials, 2013. 26(10): p. 1407-1423.

[19] Choudalakis, G. and Gotsis, A.D., Free volume and mass transport in polymer nanocomposites. Current Opinion in Colloid and Interface Science, 2012. 17(3): p. 132-140.

[20] *Gas Permeability*. [cited 2013 27 December]; Available from: http://encyclopedia2.thefreedictionary.com/Gas+Permeability.

[21] Kreiter, R., Rietkerk, M.D.A., Castricum, H.L., Veen, H.M., Ten Elshof, J.E., and Vente, J.F., Evaluation of hybrid silica sols for stable microporous membranes using high-throughput screening. Journal of Sol-Gel Science and Technology. 57(3).

[22] Yuan, Y. and Lee, T.R., *Contact Angle and Wetting Properties*, 2013, Springer Berlin Heidelberg. p. 3-34.

[23] Bunsiri, A., Somwangthanaroj, A., Samosornsuk, W., and Onsiri, Y. Prolonging shelf life and maintaining quality of straw mushroom with biodegradable plastic packaging from para rubber with consumption safe for exportation,The Office of National Research Council of Thailand and Thailand Research Fund, 2012.

[24] Zhang, C., Wang, W., Huang, Y., Pan, Y., Jiang, L., Dan, Y., Luo, Y., and Peng, Z., Thermal, mechanical and rheological properties of polylactide toughened by expoxidized natural rubber. Materials and Design, 2013. 45: p. 198-205.

[25] Ollier, R.P., Perez, C.J., and Alvarez, V.A., Preparation and characterization of micro and nanocomposites based on poly(vinyl alcohol) for packaging applications. Journal of Materials Science, 2013. 48(20): p. 7088-7096.

[26] Ishida, S., Nagasaki, R., Chino, K., Dong, T., and Inoue, Y., Toughening of Poly(L-lactide) by melt blending with rubbers. Journal of Applied Polymer Science, 2009. 113(1): p. 558-566.

[27] Kowalczyk, M. and Piorkowska, E., Mechanisms of plastic deformation in biodegradable polylactide/poly(1,4-cis-isoprene) blends. Journal of Applied Polymer Science, 2012. 124(6): p. 4579-4589.

[28] Jaratrotkamjorn, R., Khaokong, C., and Tanrattanakul, V., Toughness enhancement of poly(lactic acid) by melt blending with natural rubber. Journal of Applied Polymer Science, 2012. 124(6): p. 5027-5036.

[29] Pan, P., Kai, W., Zhu, B., Dong, T., and Inoue, Y., Polymorphous Crystallization and Multiple Melting Behavior of Poly(l-lactide): Molecular Weight Dependence. Macromolecules, 2007. 40(19): p. 6898-6905.

[30] Battegazzore, D., Bocchini, S., and Frache, A., Crystallization kinetics of poly(lactic acid)-talc composites. Express Polymer Letters, 2011. 5(10): p. 849-858.

[31] Park, J.W., Im, S.S., Kim, S.H., and Kim, Y.H., Biodegradable polymer blends of poly(L-lactic acid) and gelatinized starch. Polymer Engineering & Science, 2000. 40(12): p. 2539-2550.

[32] Smith, R., Biodegradable polymers for industrial applications. 2005, Cambridge: Woodhead Publishing Limited.

[33] Paul, D.R.a.C.B.B., Polymer blends volume1: Formulation. 2000, New Youke: John Wiley and Sons, Inc. 600.

[34] Saeidlou, S., Huneault, M.A., Li, H., and Park, C.B., Poly(lactic acid) crystallization. Progress in Polymer Science, 2012. 37(12): p. 1657-1677.

[35] Jang, W.Y., Shin, B.Y., Lee, T.J., and Narayan, R., Thermal properties and morphology of biodegradable PLA/starch compatibilized blends. Journal of Industrial and Engineering Chemistry, 2007. 13(3): p. 457-464.

[36] Schwach, E., Six, J.L., and Avérous, L., Biodegradable blends based on starch and poly(lactic acid): Comparison of different strategies and estimate of compatibilization. Journal of Polymers and the Environment, 2008. 16(4): p. 286-297.

[37] Abdul Wahab, M.K., Ismail, H., and Othman, N., Compatibilization Effects of PE-g-MA on Mechanical, Thermal and Swelling Properties of High Density Polyethylene/Natural Rubber/Thermoplastic Tapioca Starch Blends. Polymer - Plastics Technology and Engineering, 2012. 51(3): p. 298-303.

[38] Stagner, J.A., Alves, V.D., and Narayan, R., Application and performance of maleated thermoplastic starch-poly(butylene adipate-co-terephthalate) blends for films. Journal of Applied Polymer Science, 2012. 126(SUPPL. 1): p. E135-E142.

[39] Huneault, M.A. and Li, H., Morphology and properties of compatibilized polylactide/thermoplastic starch blends. Polymer, 2007. 48(1): p. 270-280.

[40] Wang, H., Sun, X., and Seib, P., Properties of Poly(lactic acid) Blends with Various Starches as Affected by Physical Aging. Journal of Applied Polymer Science, 2003. 90(13): p. 3683-3689.

APPENDIX

Appendix A

Data of Water contact angle and moisture absorption

Table A.1 Water contact angle

Sample	1	2	3	Average	SD
Neat PLA	70.59	70.72	70.96	70.76	0.19
PLA/NR 5	70.72	70.24	70.72	70.56	0.28
PLA/NR 10	73.94	73.95	73.95	73.95	0.01
PLA/NR 15	73.35	73.15	73.74	73.41	0.30
PLA/TPS 5	69.07	67.95	69.90	68.97	0.98
PLA/TPS 10	65.10	61.37	61.16	62.54	2.22
PLA/TPS 15	59.86	62.66	61.57	61.36	1.41
PLA/NR 10/TPS 5	72.1	70.96	70.24	71.11	0.95
PLA/NR 10/TPS 10	67.94	72.96	70.96	70.62	2.53
PLA/NR 10/TPS 15	66.49	68.81	70.72	68.67	2.12

Table A.2 The percentage of moisture absorption

Neat PLA Days/No.	1	2	3	Avg.	SD
1	0.1857	0.0951	0.1833	0.1547	0.0517
2	0.1901	0.2750	0.2653	0.2434	0.0464
3	0.2786	0.2852	0.2653	0.2763	0.0101
4	0.3571	0.4625	0.3537	0.3911	0.0619
5	0.2750	0.3700	0.3537	0.3329	0.0508
6	0.2852	0.5500	0.2775	0.3709	0.1551
7	0.3714	0.2750	0.3700	0.3388	0.0553
8	0.5571	0.5500	0.3537	0.4869	0.1154
9	0.2786	0.2775	0.3537	0.3032	0.0437
10	0.3714	0.3666	0.2775	0.3385	0.0529

PLA/NR5 Days/No.	1	2	3	Avg.	SD
1	0.4535	0.1109	0.1091	0.2245	0.1984
2	0.7804	0.6579	0.1091	0.4794	0.3575
3	0.5574	0.1134	0.2181	0.2963	0.2321
4	0.5574	0.4535	0.2176	0.4095	0.1741
5	0.6689	0.4535	0.6579	0.5934	0.1213
6	0.4459	0.8772	0.5453	0.6228	0.2258
7	0.2230	0.3401	0.7675	0.3704	0.1647
8	0.3344	0.3401	0.7675	0.4807	0.2484
9	0.3344	0.3401	0.4386	0.3711	0.0586
10	0.3344	0.4386	0.2181	0.3304	0.1103

PLA/NR10 Days/No.	1	2	3	Avg.	SD
1	0.2320	0.3559	0.4343	0.3407	0.1020
2	0.5800	0.7117	0.5525	0.6148	0.0851
3	0.4640	0.7117	0.5525	0.5761	0.1255
4	0.8121	0.2172	0.5525	0.5272	0.2983
5	0.4640	0.9490	0.7735	0.7288	0.2455
6	0.7092	0.6652	0.7117	0.6954	0.0262
7	0.5800	0.9456	0.4745	0.6667	0.2472
8	0.5800	1.0676	0.6630	0.7702	0.2609
9	0.5800	1.1038	0.3559	0.6666	0.3618
10	0.4640	1.2195	0.3559	0.6798	0.4705

PLA/NR15 Days/No.	1	2	3	Avg.	SD
1	0.2265	0.4367	0.4324	0.3652	0.1201
2	0.4367	0.6711	0.5488	0.5522	0.1173
3	0.5663	0.7830	0.7684	0.7059	0.1211
4	0.5663	1.0917	1.0067	0.8882	0.2821
5	1.1186	0.5405	0.5488	0.7360	0.3314
6	0.8734	0.6711	0.5643	0.7029	0.1569
7	0.4474	0.4515	0.6586	0.5192	0.1208
8	0.3398	0.7642	0.7830	0.6290	0.2507
9	0.5663	0.4474	0.7684	0.5940	0.1623
10	0.4530	0.4474	0.6486	0.5164	0.1146

PLA/TPS5 Days/No.	1	2	3	Avg.	SD
1	0.6313	0.9396	0.8130	0.3652	0.1201
2	0.8547	0.9396	0.8858	0.5522	0.1173
3	0.9497	0.9396	0.8858	0.7059	0.1211
4	0.7597	0.9396	0.6890	0.8882	0.2821
5	0.8838	0.9497	0.8054	0.7360	0.3314
6	0.8547	0.6570	0.6890	0.7029	0.1569
7	0.6711	0.7114	0.7884	0.5192	0.1208
8	0.7576	0.8547	0.7884	0.6290	0.2507
9	0.9497	0.6570	0.7874	0.5940	0.1623
10	0.8838	0.4748	1.0827	0.5164	0.1146

PLA/TPS10 Days/No.	1	2	3	Avg.	SD
1	0.9606	0.9709	1.1122	1.0146	0.0847
2	1.4409	1.5448	1.4156	1.4671	0.0685
3	1.5370	1.5534	1.5167	1.5357	0.0184
4	1.9212	1.3619	1.6178	1.6336	0.2800
5	1.7291	1.3592	1.4156	1.5013	0.1993
6	1.6330	1.4563	1.4591	1.5162	0.1012
7	1.7508	1.6505	1.5167	1.6393	0.1174
8	1.7476	1.7510	1.7189	1.7392	0.0176
9	1.5370	1.7510	1.8200	1.7027	0.1476
10	1.7508	1.5534	1.7189	1.6744	0.1060

PLA/TPS15 Days/No.	1	2	3	Avg.	SD
1	2.5759	2.5544	2.4528	2.5277	0.1550
2	6.5317	5.2259	5.0943	5.6173	0.0429
3	6.8077	7.4208	5.6604	6.6296	0.0343
4	6.1538	7.0859	5.7547	6.3315	0.1292
5	3.9735	4.2534	4.7829	4.3366	0.0722
6	7.3516	6.1320	4.4208	5.9682	0.1061
7	4.2318	4.8869	4.6944	4.6044	0.0596
8	11.3374	9.5283	7.4270	9.4309	0.0496
9	5.2980	5.1584	5.4030	5.2865	0.1466
10	3.4959	4.0681	4.2534	3.9391	0.3099

PLA/NR10/ TPS5 Days/No.	1	2	3	Avg.	SD
1	0.7735	0.6329	0.4420	0.6161	0.1664
2	0.9424	0.8574	0.8439	0.8812	0.0534
3	1.3613	1.2862	1.3713	1.3396	0.0465
4	1.3934	1.6878	1.2155	1.4322	0.2385
5	1.5470	1.6598	1.0549	1.4205	0.3217
6	1.3260	1.4523	1.2658	1.3480	0.0952
7	1.4365	1.6077	1.7932	1.6125	0.1784
8	1.6575	1.6598	1.3713	1.5628	0.1659
9	1.1050	1.5560	1.6878	1.4496	0.3056
10	1.5707	1.6598	1.1603	1.4636	0.2664

PLA/NR10/ TPS10 Days/No.	1	2	3	Avg.	SD
1	2.5343	2.1075	2.2200	2.2873	0.2212
2	2.2175	2.0182	1.8219	2.0192	0.1978
3	2.3231	2.2129	2.2200	2.2520	0.0617
4	2.3182	2.3182	2.4191	2.3552	0.0640
5	2.3231	2.3182	2.3209	2.3207	0.0025
6	2.3231	2.1075	2.5290	2.3199	0.2108
7	3.8345	3.4773	3.1377	3.4832	0.3485
8	2.7397	2.9638	2.7328	2.8121	0.1314
9	2.6344	2.2200	2.4149	2.4231	0.2073
10	3.1612	2.9505	2.9352	3.0156	0.1263

PLA/NR10/ TPS15 Days/No.	1	2	3	Avg.	SD
1	3.3238	3.4483	3.1540	3.3087	0.1477
2	3.0389	2.8156	3.2129	3.0225	0.1991
3	3.6087	3.5422	3.4323	3.5278	0.0891
4	3.6087	3.1789	3.7149	3.5008	0.2838
5	3.3575	3.3606	3.4323	3.3835	0.0423
6	3.6087	2.1789	3.9157	3.5678	0.3701
7	4.3112	4.5372	4.7310	4.5264	0.2101
8	4.3735	4.3557	4.7189	4.4494	0.2370
9	3.8936	3.6331	3.9157	3.8141	0.1572
10	3.3575	3.2698	3.8153	3.4808	0.2929

Appendix B

Data of oxygen and water permeation

Table B.1 Oxygen permeation

Sample (OP)	1	2	3	4	Avg.	SD
Neat PLA	532.658	547.361	576.081	622.517	569.652	39.587
PLA/NR5	670.126	670.049	670.073	643.475	663.431	13.304
PLA/NR10	734.369	717.802	784.996	770.376	751.886	31.127
PLA/NR15	775.516	771.908	843.192	808.778	799.848	33.322
PLA/TPS5	589.149	579.333	626.085	597.113	597.920	20.135
PLA/TPS10	487.921	483.632	499.043	496.112	491.677	7.136
PLA/TPS15	463.635	484.173	451.000	465.603	466.103	13.674
PLA/NR10/TPS5	679.700	624.784	644.066	662.948	652.874	23.719
PLA/NR10/TPS10	703.019	728.224	667.575	698.128	699.236	24.888
PLA/NR10/TPS15	728.038	694.572	687.583	755.853	716.512	31.616

Table B.2 Water vapor permeation

Sample (WVP)	1	2	3	Avg.	SD
Neat PLA	184.189	186.110	182.252	184.184	1.929
PLA/NR5	199.102	196.693	200.819	198.871	2.073
PLA/NR10	203.685	198.258	202.803	201.585	2.907
PLA/NR15	207.638	207.008	206.394	207.013	0.622
PLA/TPS5	246.315	234.268	236.535	239.039	6.402
PLA/TPS10	254.803	237.480	277.591	256.624	20.117
PLA/TPS15	303.370	294.677	316.110	304.719	10.780
PLA/NR10/TPS5	213.087	212.378	252.961	212.732	0.501
PLA/NR10/TPS10	225.528	230.142	215.9528	223.874	7.23757
PLA/NR 10/TPS 15	256.835	247.339	248.6299	250.9344	5.150409

Appendix C

Data of mechanical properties

Table C.1 Mechanical properties in MD of neat PLA

No.	Tensile strength (MPa)	Young's modulus (MPa)	Elongation at break (%)	Tensile toughness (mJ)
1	91.28	4100.75	4.07	111.12
2	91.14	4143.06	3.87	98.89
3	91.87	4138.17	2.49	53.46
4	91.54	4125.12	2.66	55.72
5	91.95	4121.91	2.52	53.22
Avg.	91.56	4125.80	3.12	74.48
SD	0.36	16.54	0.78	28.21

Table C.2 Mechanical properties in MD of PLA/NR5

No.	Tensile strength (MPa)	Young's modulus (MPa)	Elongation at break (%)	Tensile toughness (mJ)
1	67.52	3642.06	11.66	263.57
2	68.68	3630.92	11.40	228.45
3	70.28	3673.00	16.26	311.23
4	67.55	3625.84	14.01	202.32
5	67.04	3647.80	9.99	284.49
Avg.	68.70	3643.92	12.66	258.01
SD	1.03	18.44	2.47	43.41

Table C.3 Mechanical properties in MD of PLA/NR10

No.	Tensile strength (MPa)	Young's modulus (MPa)	Elongation at break (%)	Tensile toughness (mJ)
1	56.83	3292.54	19.00	342.20
2	55.59	3255.34	15.44	268.79
3	52.15	3229.99	11.00	182.86
4	53.58	3259.65	15.19	224.29
5	55.00	3246.19	20.34	329.95
Avg.	54.63	3256.74	16.19	282.22
SD	1.81	23.02	3.66	85.54

Table C.4 Mechanical properties in MD of PLA/NR15

No.	Tensile strength (MPa)	Young's modulus (MPa)	Elongation at break (%)	Tensile toughness (mJ)
1	44.12	3138.47	9.30	128.16
2	46.13	3195.24	8.85	117.77
3	45.67	3130.07	9.14	105.18
4	46.77	3256.00	9.90	124.20
5	46.52	3257.70	8.72	124.11
Avg.	45.84	3195.50	9.12	119.88
SD	1.05	61.37	0.53	9.02

Table C.5 Mechanical properties in MD of PLA/TPS5

No.	Tensile strength (MPa)	Young's modulus (MPa)	Elongation at break (%)	Tensile toughness (mJ)
1	72.57	4041.66	2.59	49.08
2	71.34	3992.75	2.61	45.14
3	72.97	4042.91	2.50	46.36
4	70.29	4086.93	2.51	46.85
5	70.21	4022.97	2.49	48.62
Avg.	71.48	4037.44	2.54	47.21
SD	1.27	34.29	0.06	1.63

Table C.6 Mechanical properties in MD of PLA/TPS10

No.	Tensile strength (MPa)	Young's modulus (MPa)	Elongation at break (%)	Tensile toughness (mJ)
1	53.26	3298.92	2.44	41.70
2	53.78	3358.50	2.33	35.20
3	54.40	3388.83	2.28	39.15
4	52.88	3301.19	2.56	38.21
5	54.63	3429.81	2.49	38.89
Avg.	53.79	3322.38	2.42	38.63
SD	0.74	50.18	0.11	2.33

Table C.7 Mechanical properties in MD of PLA/TPS15

No.	Tensile strength (MPa)	Young's modulus (MPa)	Elongation at break (%)	Tensile toughness (mJ)
1	53.73	3192.17	2.41	39.78
2	51.48	3270.55	2.46	37.65
3	55.77	3217.19	2.49	38.06
4	53.91	3290.84	2.56	38.99
5	52.91	3234.22	2.56	37.76
Avg.	53.56	3240.99	2.50	38.45
SD	1.57	39.86	0.07	0.91

Table C.8 Mechanical properties in MD of PLA/NR10/TPS5

No.	Tensile strength (MPa)	Young's modulus (MPa)	Elongation at break (%)	Tensile toughness (mJ)
1	53.16	3281.11	2.89	43.30
2	53.32	3292.33	3.69	57.32
3	52.62	3247.51	2.81	43.79
4	52.70	3283.21	2.76	40.37
5	52.84	3271.93	3.08	46.88
Avg.	52.93	3275.02	3.05	46.33
SD	0.30	16.99	0.38	6.56

Table C.9 Mechanical properties in MD of PLA/NR10/TPS10

No.	Tensile strength (MPa)	Young's modulus (MPa)	Elongation at break (%)	Tensile toughness (mJ)
1	45.32	2934.64	2.53	35.88
2	44.80	2985.53	2.56	38.30
3	44.36	2958.88	2.78	37.91
4	44.34	2994.67	2.73	37.53
5	45.24	2967.91	2.77	37.02
Avg.	44.81	2968.33	2.67	37.33
SD	0.46	23.53	0.12	0.94

Table C.10 Mechanical properties in MD of PLA/NR10/TPS15

No.	Tensile strength (MPa)	Young's modulus (MPa)	Elongation at break (%)	Tensile toughness (mJ)
1	35.70	2494.21	3.39	36.86
2	36.51	2446.95	3.01	36.77
3	35.26	2431.96	3.12	32.87
4	35.21	2434.84	3.01	33.75
5	26.64	2488.13	3.43	33.67
Avg.	35.86	2459.22	3.19	34.78
SD	0.68	29.78	0.20	1.89

Table C.11 Mechanical properties in TD of neat PLA

No.	Tensile strength (MPa)	Young's modulus (MPa)	Elongation at break (%)	Tensile toughness (mJ)
1	74.54	4114.11	3.37	70.54
2	74.50	4126.53	2.81	56.24
3	74.56	4075.01	2.19	39.98
4	74.65	4039.34	2.78	56.18
5	74.46	4140.96	3.23	69.18
Avg.	74.54	4099.19	2.88	58.42
SD	0.07	41.48	0.47	12.38

Table C. 12 Mechanical properties in TD of PLA/NR5

No.	Tensile strength (MPa)	Young's modulus (MPa)	Elongation at break (%)	Tensile toughness (mJ)
1	51.57	3523.47	15.15	91.14
2	50.98	3524.32	13.13	142.60
3	51.72	3543.09	8.55	160.96
4	50.05	3579.09	10.26	100.02
5	50.03	3558.11	12.23	128.01
Avg.	50.87	3545.78	11.86	124.55
SD	0.81	23.58	2.55	29.07

Table C.13 Mechanical properties in TD of PLA/NR10

No.	Tensile strength (MPa)	Young's modulus (MPa)	Elongation at break (%)	Tensile toughness (mJ)
1	40.55	3097.90	15.21	222.52
2	40.30	3045.10	12.80	163.57
3	41.91	3177.80	17.26	217.69
4	41.47	3065.40	14.97	184.71
5	40.08	3126.40	12.06	152.71
Avg.	40.86	3102.52	14.46	188.16
SD	0.79	52.28	2.08	31.44

Table C.14 Mechanical properties in TD of PLA/NR15

No.	Tensile strength (MPa)	Young's modulus (MPa)	Elongation at break (%)	Tensile toughness (mJ)
1	32.79	3056.70	9.90	111.60
2	32.82	3050.50	10.04	110.52
3	32.22	3047.10	9.40	109.25
4	32.77	3064.00	10.59	102.52
5	32.72	3096.00	9.16	108.91
Avg.	32.66	3062.86	9.82	108.56
SD	0.25	19.61	0.56	3.54

Table C.15 Mechanical properties in TD of PLA/TPS5

No.	Tensile strength (MPa)	Young's modulus (MPa)	Elongation at break (%)	Tensile toughness (mJ)
1	55.07	3920.69	1.65	20.42
2	55.26	3942.37	1.64	20.26
3	55.18	3932.85	1.69	20.84
4	54.59	3933.02	1.62	21.40
5	54.77	3966.33	1.66	21.23
Avg.	54.97	3939.05	1.65	20.83
SD	0.28	17.08	0.03	0.49

Table C.16 Mechanical properties in TD of PLA/TPS10

No.	Tensile strength (MPa)	Young's modulus (MPa)	Elongation at break (%)	Tensile toughness (mJ)
1	47.33	3618.95	1.48	18.05
2	47.32	3645.56	1.62	17.00
3	47.42	3690.56	1.50	16.40
4	50.71	3689.02	1.57	17.36
5	47.09	3622.00	1.52	15.09
Avg.	47.97	3653.22	1.54	16.78
SD	1.53	34.94	0.06	1.12

Table C.17 Mechanical properties in TD of PLA/TPS15

No.	Tensile strength (MPa)	Young's modulus (MPa)	Elongation at break (%)	Tensile toughness (mJ)
1	50.21	3368.61	1.53	15.32
2	50.63	3390.44	1.47	14.54
3	50.18	3277.51	1.53	13.32
4	49.44	3343.63	1.41	15.97
5	50.23	3330.89	1.47	14.32
Avg.	50.14	3342.22	1.48	14.52
SD	0.43	42.83	0.05	1.16

Table C.18 Mechanical properties in TD of PLA/NR/10/TPS5

No.	Tensile strength (MPa)	Young's modulus (MPa)	Elongation at break (%)	Tensile toughness (mJ)
1	42.20	3209.95	2.31	27.89
2	40.83	3111.61	2.36	27.80
3	41.22	3113.29	2.30	26.22
4	42.28	3130.40	2.14	24.14
5	40.88	3136.63	2.11	24.02
Avg.	41.48	3140.38	2.24	26.01
SD	0.71	40.36	0.11	1.89

Table C.19 Mechanical properties in TD of PLA/NR/10/TPS10

No.	Tensile strength (MPa)	Young's modulus (MPa)	Elongation at break (%)	Tensile toughness (mJ)
1	38.69	2871.09	2.42	27.33
2	39.67	2915.66	2.41	27.72
3	38.72	2916.69	1.96	20.51
4	39.30	2956.05	2.27	24.31
5	38.65	2949.73	2.16	23.67
Avg.	39.01	2921.84	2.24	24.71
SD	0.45	33.87	0.19	2.95

Table C.20 Mechanical properties in TD of PLA/NR/10/TPS15

No.	Tensile strength (MPa)	Young's modulus (MPa)	Elongation at break (%)	Tensile toughness (mJ)
1	33.17	2396.80	2.26	23.44
2	33.63	2373.09	2.22	23.59
3	33.16	2384.57	2.20	21.00
4	33.25	2324.18	2.31	23.00
5	34.16	2311.35	2.16	22.79
Avg.	33.47	2358.00	2.23	22.76
SD	0.43	37.94	0.06	1.04

Appendix D

Data of impact and tear strength

Table D.1 Impact strength of binary blends (PLA/NR)

Impact strength	Neat PLA	PLA/NR5	PLA/NR10	PLA/NR15
1	3.94	6.25	22.66	16.04
2	3.94	5.54	23.40	16.78
3	3.94	5.54	23.35	17.56
4	3.94	6.25	21.84	17.65
5	3.94	6.25	23.71	17.65
Avg.	3.94	5.97	22.99	17.14
SD	0.00	0.39	0.75	0.71

Table D.2 Impact strength of binary blends (PLA/TPS)

Impact strength	PLA/TPS5	PLA/TPS10	PLA/TPS15
1	3.84	3.75	3.14
2	3.84	3.14	3.14
3	3.84	3.14	3.14
4	3.84	3.14	3.14
5	3.84	3.75	3.14
Avg.	3.84	3.38	3.14
SD	0.00	0.34	0.00

Table D.3 Impact strength of ternary blends (PLA/NR/TPS)

Impact strength	PLA/NR10/TPS5	PLA/NR10/TPS10	PLA/NR10/TPS15
1	12.18	12.84	12.88
2	12.84	10.83	10.42
3	14.86	13.50	12.25
4	10.13	11.49	8.59
5	14.20	8.77	7.36
Avg.	12.71	11.49	10.30
SD	1.88	1.85	2.35

Table D.4 Tear strength of binary blends (PLA/NR) in MD and TD

Sample	Tear strength (Nm)	
	MD	TD
Neat PLA	684.90 ± 0.00	913.00 ± 0.00
PLA/NR5	721.00 ± 0.00	961.00 ± 0.00
PLA/NR10	782.80 ± 0.00	1043.00 ± 0.00
PLA/NR15	1106.00 ± 0.00	1382.00 ± 0.00

Table D.5 Tear strength of binary blends (PLA/TPS) in MD and TD

Sample	Tear strength (Nm)	
	MD	TD
PLA/TPS5	684.90 ± 0.00	913.00 ± 0.00
PLA/TPS10	456.60 ± 0.00	668.20 ± 0.00
PLA/TPS15	456.60 ± 0.00	652.30 ± 0.00

Table D.6 Tear strength of ternary blends (PLA/NR10/TPS) in MD and TD

Sample	Tear strength (Nm)	
	MD	TD
PLA/NR10/TPS5	782.80 ± 0.00	1043.00 ± 0.00
PLA/NR10/TPS10	936.40 ± 0.00	1170.00 ± 0.00
PLA/NR10/TPS15	702.50 ± 0.00	936.40 ± 0.00

VITA

Miss Nuengruthai Jaitrong was born on November 6, 1987 in Trat, Thailand. She finished high school at Dara Academy, Chiang Mai. In 2010, she received the Bachelor's Degree from Department of Chemical Engineering, Faculty of Engineering, Thammasat University. She continued her study for Master's Degree in Chemical Engineering at the Department of Chemical Engineering, Faculty of Engineering, Chulalongkorn University in June, 2011.

She participated in poster presentation in the title of "Effect of Poly(lactic acid) /Natural Rubber/Thermoplastic Starch Blown Films on Morphology, Gas Permeability and Mechanical Properties", During January 8-10, 2014 at Pure and Applied Chemistry International Conference 2014 in Khon Kaen, Thailand. Additionally, she received the certificate for outstanding poster presentation in this conference.